CHALMERS
UNIVERSITY OF TECHNOLOGY

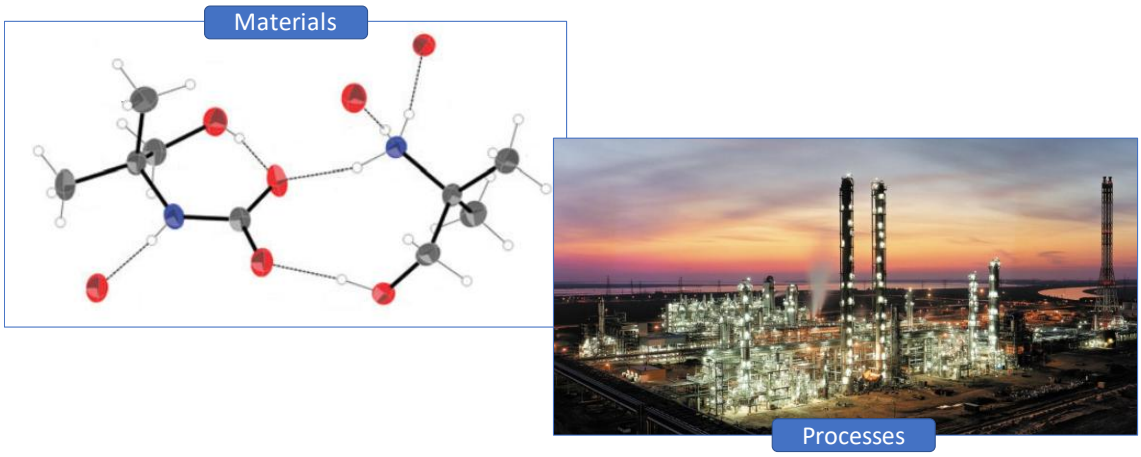

Modelling of an Amine-Organic Solvent based Carbon-Capture Process for Efficient Excess Heat Utilization

Master's thesis in Innovative and Sustainable Chemical Engineering

RUTH GARCIA CALLE

Department of Space, Earth and Environment - Division of Energy Technology
CHALMERS UNIVERSITY OF TECHNOLOGY
Gothenburg, Sweden 2018

Master's thesis 2018

Modelling of an Amine-Organic Solvent based Carbon-Capture for Efficient Excess Heat Utilization

Ruth Garcia Calle

CHALMERS
UNIVERSITY OF TECHNOLOGY

Department of Space, Earth and Environment
Division of Energy Technology
Chalmers University of Technology
Gothenburg, Sweden 2018

Modelling of an Amine-Organic Solvent based Carbon-Capture for Efficient Excess Heat Utilization

RUTH GARCIA CALLE

Supervisor: Max Biermann

Examiner: Assistant Professor Dr. Fredrik Normann

Master's Thesis 2018
Department of Space, Earth and Environment
Division of Energy Technology
Combustion and Carbon Capturing Technologies
Chalmers University of Technology
SE-412 96 Gothenburg
Telephone +46 31 772 1000

Printed by Reproservice
Gothenburg, Sweden 2018

Acknowledgement

I want to express my gratitude to my supervisor, Max Biermann, for having always time for discussing anything in my mind; for teaching me how to embrace comments. To my examiner, Fredrik Normann, for the countless efforts put in the system chemistry. I thank both for the possibility to develop this Master's thesis.

I am grateful for the time I spent at the Faculty of Engineering at Lund University. I want to thank Helena Svensson for counting me as another member of her team. I acknowledge Meher Sanku, for her invaluable support and her vision; Hanna Karlsson, for her positive and helpful attitude and the three of them for the great experimental work.

I praise my parents, Julián and Teresa, who have always believed in me and supported me during my Master studies. I could have never accomplished this much without you two. I am grateful to my sister, Itziar, for cheering me up when I needed a smile.

Ernesto, thank you for simply being there for me, I am so lucky to have you.

I thank my friends. Giulia and Badhri, I cannot imagine better partners for this 2-year adventure. Gabriela thanks for all your experienced advice. To my gym buddies, Nelly and Andrea, for being part of my fun stress release.

Gothenburg, June 11

Ruth Garcia Calle

Abstract

The vast emissions of CO_2, the major cause of global warming, have to be addressed to meet the target to keep the global temperature increase relative to pre-industrial levels to below 2 °C. For existing emission-intensive industrial sites, a retrofit with post-combustion capture of CO_2 and subsequent geological storage is an attractive option. Post-combustion processes based on chemical absorption are considered state of the art for carbon capture due to its extensive use in oil & gas industry and have been demonstrated in large scale. However, the costs associated with investment, solvent regeneration, carbon dioxide compression and required geological sequestration have prevented its deployment so far.

This Master's thesis develops a process model for a novel post-combustion carbon capture system based on a solution of 2-amino-2-methyl-1-propanol (AMP) in the organic solvent N-methyl-2-pyrrolidine (NMP). This is a precipitating system forming solid carbamate, which can be separated prior to regeneration to reduce the amount of material to be heated. The solvent has shown potential in lab-scale experiments to reduce the cost for the heat required for regeneration and for the compression work. The major advantage is the low temperature (70-90 °C) required for regenerating the AMP-NMP solvent - aqueous monoethanolamine (MEA), which is the benchmark solvent, commonly requires 120 °C. This feature may allow for increased utilization of low-value excess heat to power the solvent regeneration.

The model includes property data suitable for the organic solvent derived from experimental data. The model of the absorption process is designed to be able to describe the solid formation, which is an important part of this process. The model was adjusted to represent reality as close as possible and it follows expected trends when testing it for sensitivity towards key process parameters.

The process model has been used to evaluate its performance and the sensitivity towards key process parameters. The process performance was compared to that of the benchmark MEA-process. Two cases were considered. The MEA-process is better for a constant CO_2 capture rate of 90% from the steel-mill blast-furnace gas as it requires lower solvent circulating, smaller absorption column, and lower specific heat demand. The second case is an oil refinery, where the capture rate is adjusted so that only excess-heat at the corresponding reboiler temperatures is utilized to power the solvent regeneration. In this case, the higher amounts of excess-heat available at the lower reboiler temperature of AMP-NMP overcome the higher specific heat demand and the AMP-NMP outperforms the MEA process in terms of percentage of CO_2 captured. In summary, the most important application for the AMP-NMP process is the possibility for efficient partial carbon capture when regeneration is driven by low-value excess heat.

Contents

List of figures

List of tables

1. Introduction

1.1. Background

The commitment to keep temperature increase on the planet below 2 °C above pre-industrial levels has put a spotlight on the need for carbon capture and storage (CCS) technologies. Post combustion capture is considered as state of the art, but new processes designs and solvents are currently desired to increase cost effectiveness. Solvent regeneration and outlet carbon dioxide stream compression are known to be the most expensive stages in post combustion capture. Solvent regeneration through low-value excess heat utilization is one of the most promising alternatives for low cost CCS application in the process industry [1]. The application to emission intensive industries, such as iron and steel, cement, petroleum refineries and pulp and paper industries has been investigated.

Some processes have even been commercialized, such as the amine based Cansolv Carbon Dioxide (CO_2) Capture System by Shell. However, CCS application is still low due to the lack of more economical alternatives. One of the reasons behind this is the wide variety of conditions existing within the process industry. Carbon concentration, quantity and availability of excess heat affect the process configuration and economy. Each case is different and processes would need to have specific adjustments.

Most known absorption processes employ conventional solvents like ammonia and its organic derivatives, amines, such as aqueous solutions of monoethanolamine (MEA). The types of amines considered as solvent include sterically hindered amines. In general, the use of this sort of amines provides high absorption capacity, rate, selectivity as well as resistance to degradation for CO_2 capture [2]. In addition to this, the component formed through the chemical absorption in an organic solvent based system is less stable than the corresponding to reaction with conventional amines, which can reduce the energy required for the regeneration. Another factor that could be related to the use of new solvents is the possibility for pressurized solvent regeneration, which reduces the need for CO_2 compression. In this way, the two most costly aspects could be addressed.

This Master's thesis considers the possible application of a new solvent. The solvent is the hindered amine 2-amino-2-methyl-1-propanol, AMP, in an organic solution of N-methyl-2-pyrrolidone (NMP). Specifically, in this system, chemical absorption leads to solid precipitation. When employing organic solvents, carbamate has been reported as the solid precipitate [3]–[6]. The solvent regeneration of this new system can be achieved at 55-90 °C, compared to 120 °C generally required for aqueous MEA solutions [3]. This fact increases process integration possibilities using low-value waste heat in the regeneration stage. When modifying the regeneration temperature of the AMP-NMP, the pressure of the CO_2 stream leaving the system can also be varied [7]. The pressure-temperature relationship will thus require cost optimization between the possibilities for cost decrease in the compression stages versus the higher temperatures required for solvent regeneration.

Figure 1 shows a simplified CCS process overview for AMP-NMP system. It includes a filtering stage for the solid precipitate and since it differs from common processes, it is important to recognize several streams. Lean is the stream entering the absorber; rich, the one leaving; solid concentrated - also referred as retained solid - is the stream going to regeneration after splitting through filtering and regenerated is the one leaving the stripper.

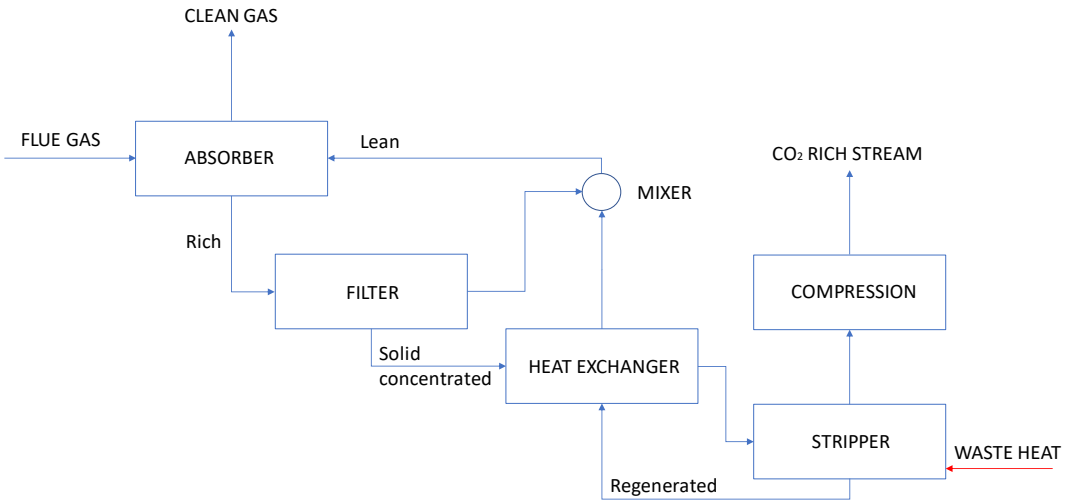

Figure 1. Flowsheet highlighting the possibilities for low-value waste heat integration for AMP-NMP system

1.2. Aim

This work develops a model for the AMP/NMP solvent system and evaluates it for carbon capture relative to the benchmark - the aqueous MEA based system. The work focuses on carbon capture from process industries and the utilization of available excess heat. Furthermore, the scalability and applicability to certain industrial sectors - iron&steel and oil&gas - of the AMP/NMP solvent is analysed. The work utilizes evaluation of experimental data on the solvent performance previously derived at Lund University to determine component, process design and simulation in Aspen Plus^{TM} and testing process implementation in emission-intensive industries through case studies.

2. State of the art

2.1. Environmental impact assessment

The main contributor to global warming is considered to be the rise in CO_2 emissions [8]. Concentrations in the atmosphere were found to be 400 ppm in November 2015 [9]. If no measures or actions are taken towards its mitigation, the CO_2 concentration is expected to increase up to 600-1550 ppm by 2030 [10]. This situation would result in a temperature increase in 4.1-4.8°C from pre-industrial levels by the end of the 21st century. To face this situation, 195 nations subscribed the agreement to *"combat climate change and unleash actions and investment towards a low carbon, resilient and sustainable future"* at the 21st Conference of the Parties (COP21) held in Paris between 30th November and 11th December 2015 [11], [12]. Mitigation scenarios resulting from it, aim for a 2°C increase limit, corresponding to a CO_2 concentration under 450 ppm (v) [9], [13] .

World Meteorological Organization (WMO) confirmed 2017 to be part of the top three hottest years, with an average surface temperature 1.1°C increase from pre-industrial levels. Moreover, WMO will be publishing a full Statement on the State of Climate where a further overview will include temperature variability and trends, high-impact events as well as long-term indicators of climate change. Among these, sea ice both in Arctic and Antarctic regions, sea level rise, ocean acidification and carbon dioxide concentration levels will be included [14].

2.1.1. Mitigation technologies

There exist several alternatives to control and diminish CO_2 emissions. Some of these can be drawn from energy efficiency improvements, substituting current fuels by less intensive ones, using renewable energy sources and applying carbon capture and storage (CCS) [15]. Most scenarios consider a mixture of technologies is required to accomplish the concentration limit target [13], [16]–[19].

Fossil fuels are expected to continue to be the main energy source for the upcoming 50 years [20]. CCS has a special value since it accomplishes emission reduction without disturbing the current infrastructure and preserves the value of fossil fuel reserves [21], [22]. This is the reason why it is expected to greatly contribute in emission reduction in power generation and industrial application processes, such as cement, iron and steel, oil refining, pulp and paper and biofuels sectors [23].

The joint use of CCS and biomass (BioCCS) has been gaining attention due to its associated negative emissions. This potential is considered specially to compensate for those industries in which it would be too costly or hard to implement any technology to reduce its emissions [13]. In reality, most mitigation scenarios considered include this technology, which has not been proven in the large scale, to achieve emissions reduction pathways [15], [17].

Most scenarios that attempt to fulfil the limit set without CCS have been found not to converge. In fact, from the different abatement strategies, CCS has been found to be the costliest alternative to be replaced by a counterpart [13], [19]**.** However, so far, CCS's cost is still limiting its large-scale application [24]. Since capturing accounts for 70 to 80% of the total costs, the main research efforts are devoted to this process stage [10].

Even though CCS is considered an effective technology towards climate change mitigation, it also presents certain adverse effects. When applied in power plants, efficiency is lowered or fuel consumption increased. In addition to this, the cooling utility requirements are also increased, so is the electricity and chemicals consumption [15]. Additional infrastructure would be also required to transport the CO_2 and store it, leading to an increase in direct non-CO_2 emissions and in indirect CO_2 and other emissions.

2.2. Carbon capture

CCS cover technologies in which CO_2 is selectively removed from gas streams to be compressed into supercritical conditions for its transportation and sequestration in certain geologic formations, such as depleted oil and gas reservoirs and oceans [25].

2.2.1. Process classification

Within the capture stage in CCS, three main categories can be differentiated: post-combustion, pre-combustion and oxy-fuel [26], [27]. Schematic processes are shown in Figure 2. The preferred technology is mostly determined by the fuel type, CO_2 partial pressure and overall stream pressure, as well as the industrial process generating the CO_2.

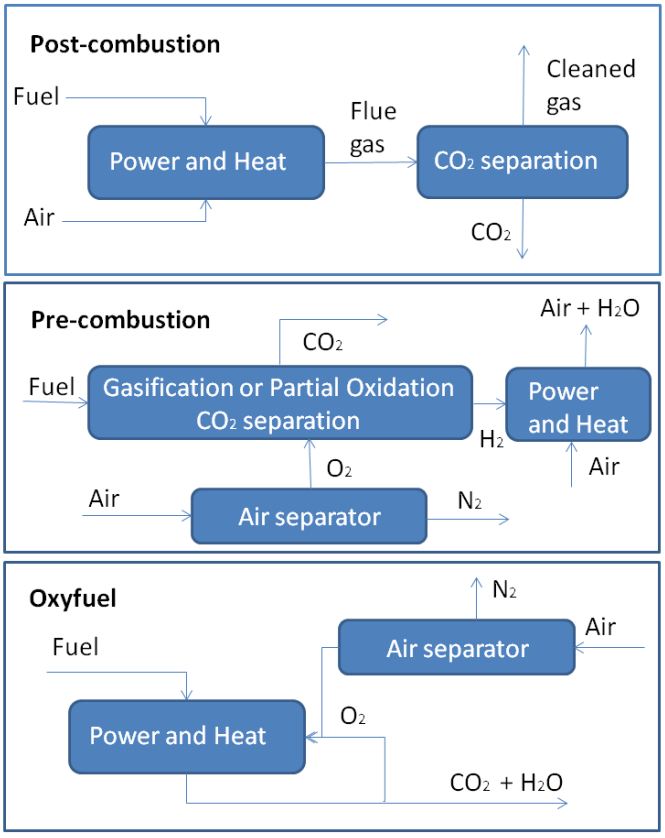

Figure 2. Carbon capture approaches and technology options [28]

Post-combustion processes directly extract the CO_2 from flue gas streams [24]. It usually involves chemical absorption and it is preferred when CO_2 partial pressure is low. For solvent regeneration, a temperature swing is employed to release the CO_2 from the solvent.

Pre-combustion processes convert the fuel into syngas employing air or oxygen. Later, the mixture undergoes a water-gas shift reaction in which CO is further oxidized into CO_2, with

additional H_2 formation which can be burnt with zero-emission of CO_2 [9]. Partial pressure of CO_2 is therefore increased which allows for its capture with a physical solvent. This can be regenerated through pressure swing, instead of the temperature swing employed in the post-combustion processes, which is a much less energy intensive alternative [15].

Oxy-fuel refers to those processes in which pure oxygen is used instead of air in the combustion stage. Exhaust gas is, in this case, mainly composed of steam and CO_2, which can be separated. Further purification may be required for the CO_2 stream [15].

From these, a promising alternative is post combustion based on chemical absorption due to the familiarity of the technologies involved, the easier retrofitting of already existing plants and the fact that it is a proven technology, meaning there have been projects demonstrating its applicability [12].

2.2.2. Technological alternatives for post-combustion capture

Several capture routes have been investigated over the past decades, some of which are presented in this section.

2.2.2.1.Absorption based CO_2 capture

Absorption, by chemical or physical means, to capture CO_2 has been employed in post-combustion and pre-combustion approaches, respectively. In the first case, aqueous ammonia, amine based solvents and alkaline solutions are mostly used [29]–[32]. In the latter, several commercial well-established processes are available such as Selexol, Rectisol, Purisol or Fluor.

Absorption is a well-known separation method with high capture efficiency. All concepts are similar, including CO_2 absorption stage and solvent regeneration which is accomplished by stripping. A schematic process is shown in Figure 3. Solvent regeneration induces a high energy penalty [33]. This could, to some extent, be reduced in industries where heat integration was possible. In addition to this, absorption based processes present other drawbacks such as corrosion or large volume water make-up requirements. Solvent poisoning from impurities in the flue gas stream may also become a major issue, reducing solvent's stability [24]**.**

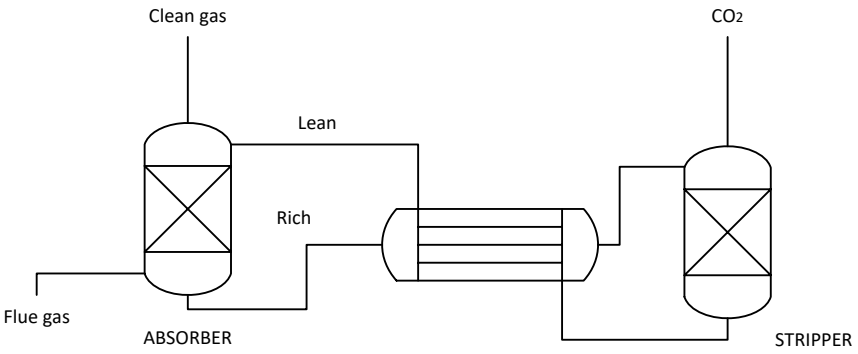

Figure 3. Post-combustion carbon capture process based on MEA chemical absorption [28]

Next generation of absorption processes should include process configurations improvements, providing heat integration involving for example inter-heated strippers to improve heat recovery in the stripper overhead or inter-cooled absorbers, increasing reversibility in the absorption stage with greater rich and lean loadings [24].

2.2.2.2.Membrane based CO_2 capture

Membranes represent energy efficient and environmentally friendly alternatives for CO_2 capture. The flow is driven by a permeation process due to the pressure difference across the membrane. Membrane configuration, material, morphology and composition as well as operating conditions are considered the main factors affecting the separation performance [24]. The use of membrane separation in post-combustion processes presents certain challenges of which the most important would be the low pressure in the flue gas streams.

Comparing to other capturing routes, membrane operation would involve multistage operation and streams recycling, which may be challenging due to the increased operation complexity and difficulty [24].

2.2.2.3.Adsorption based CO_2 capture

Capital cost for CO_2 adsorption on solid surfaces would still be generally high due to the large volumes of flue gas to be treated and the use of expensive adsorbents may implicate economical unfeasibility in the large scale [28]. Both efficiency and process economy in pressure and temperature swing adsorption (PSA/TSA) are affected by adsorbent characteristics, process design and operation factors [34], [35]. Adsorbent should fulfil certain characteristics to withstand scale up, such as high working capacity and selectivity, low cost, low regeneration requirements, long-term stability, especially to adsorption/desorption cyclic process, and fast kinetics [10], [28], [36]. Some of the process design factors and conditions that should be optimized include cycle configuration, numbers of steps and beds, cycle time and operating pressures/temperatures [24].

PSA technologies have attracted lots of attention lately due to their lower energy requirements and costs, as well as the simplicity in the process [37]. Its low CO_2 recovery remains though as a challenge to be overcome [35]. When considering post-combustion alternatives, vacuum swing adsorption (VSA) and TSA remain to be more appropriate, mainly since PSA incurs much larger pressure drops in flue gas applications [38]–[41].

When comparing technology limitations, adsorption processes can overcome most of the ones present in absorption based ones. However, adsorption processes are far from being cost effective, at least up to the current state of development. Moreover, these technologies have not been yet proven in large scale application [42]–[44]. Development of alternatives in relation to design, optimization and adsorbents performance evaluation should be coupled with the actual practical application and process conditions considered [24].

2.2.2.4.CO_2 capture by chemical looping

Chemical looping combustion and reforming, CLC and CLR respectively, are potential cost-effective process alternatives for CO_2 capture. An additional advantage is the reduction in NO_x compounds formation. Even valuable by-products can be obtained with these technologies, for example when combining CLC and IGCC, syngas is obtained [24].

A metal oxide acts as energy carrier between air and fuel reactors. Therefore, there exists a need for this kind of compounds when considering its scalability. The potential candidates should fulfil certain criteria, of which high oxidation/reduction activity is the most important.

They should also present mechanical and long-term stability, resistance to agglomeration, high melting point, low cost and environmental impact [45].

Most chemical looping technologies are still under concept or lab scale development, with few in pilot-scale [46]–[48]. Its full availability for actual application is not expected before 2030 [23].

To summarize, capturing technologies with their associated challenges and opportunities are presented in Table 1.

Table 1. Technologies, challenges and opportunities within CCS capturing stage [24]

Capture technology	Challenges	Opportunities
Absorption	Equipment corrosion Amine degradation High regeneration energy requirement High overall energy penalty Environmental impact	Improvement in commercially available absorption technologies The use of ionic liquids (ILs) The use of advanced amines
Membrane	Energy intensive for post-combustion application High fabrication cost of novel membranes Not suitable for high-temperature applications Trade-off between purity and recovery Low selectivity	Composite hollow-fiber membranes MMMs Hybrid membrane–cryogenic processes
Adsorption	Long-term stability to impurities and moisture Thermal management pressure-drop and adsorbent attrition	Composite adsorbents Structured adsorbents Rapid swing cycles
Chemical looping	High-pressure operation Efficient and stable oxygen-carrier materials	Composite oxides as oxygen carriers Process-design modifications

2.3. Chemical absorption based CO_2 capture

Developing post-combustion CCS based on chemical absorption provides certain advantages such as retrofitting of already existing plants with minimum modifications and relying on already well-known and established technologies [49], [50]. Figure 4 presents the technology readiness level (TRL), which is a method to assess, in a scale 1-9, the maturity level of certain technologies.

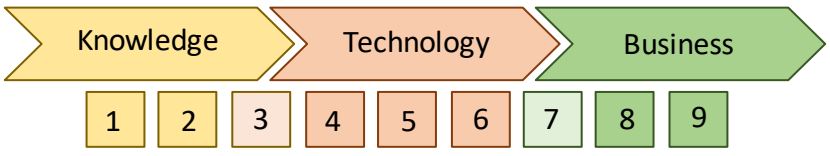

Figure 4. Technology readiness levels [51]

Even though costs for chemical absorption based CCS, both capital and operating, continue to be higher than what could be acceptable, TRL for these processes is within 6-8 [50]. Therefore, as it can be withdrawn from Figure 4, these sorts of processes are already somewhere between pilot plan, scale up and initial market launch and commercialisation stages, e.g. research at pilot plant level has focused on several factors such as different solvents, scale-up procedures, solvent degradability, corrosion, operation and process energy efficiency [52]–[60]. Academia and between industries collaborations are observed in facilities such as the European CO_2 Test Centre Mongstad (TCM) in Norway, where ammonia and amine based processes are tested [61]. It was developed by Gassnova, Statoil, Sasol and Shell and some of the current commercially available processes have been tested in it, such as Shell's CanSolv or Alstom's Chilled Ammonia Process (CAP) among others [49].

2.3.1. Process configurations

Alternative process configurations have been considered by including extra equipment. These have proven to be, via thermodynamic analysis, generally more energy efficient than the original conventional configuration [49]. Comparison between sixteen different process configurations to prove the potential for energy savings was presented in [62]. However, no direct conclusions could be withdrawn since some alternatives run with different solvents, targets for acid gas removal and operating conditions. Thus, ten process configurations were studied under common settings in [63].

2.3.2. Solvents

Chemicals to be employed as solvents in absorption based processes ideally possess the following properties [64].

- High CO_2 capacity
- High absorption rate
- Low vapour pressure
- Low viscosity
- Low cost
- Non-corrosive behaviour
- No degradation in operating conditions
- Non-toxic
- Non-hazardous

Common solvents include amines, the organic ammonia derivatives. Depending on the degree of hydrogen substitution by organic groups, amines can be classified in primary, secondary and tertiary. There are also sterically hindered amines for which two varieties exit i) primary amines with the amine group linked to a tertiary carbon and ii) secondary amines with the amine link with a secondary or tertiary carbon [65].

From Table 2, it is possible to realize sterically hindered amines present certain advantages and disadvantages regarding the ideal properties highlighted before [2].

Table 2. Solvent properties summary for amines, alkali salts and ammonia [64]

	Heat of absorption	Absorption rate	Capacity	Degradation tendency
Primary	High	High	Medium	High
Secondary	High	Medium	Medium	Medium
Tertiary	Medium	Low	High	Low
Sterically hindered	High	Medium	High	Low
Polyamines	High	High	Medium	Low
Alkali salts	Low	Low	High	Low
Ammonia	Medium	Medium	High	Low

The benchmark solvent for post-combustion carbon capture is MEA with up to 30% concentration in weight. Several features justify its use, such as the rapid kinetics [66]. However, its high regeneration energy combined with the large solvent circulation rates leads to high energy consumptions. In addition to this, CO_2-MEA mixtures are highly corrosive and degrade quickly [49]. These are certain drawbacks regarding its use and the basic reasons behind new solvent development for post-combustion CCS.

Within new solvent development, certain categories can be distinguished such as mixed amine-based, ammonia-based, amino acid based, biphasic and ionic-liquid based solvents [25], [67]–[71]. Biphasic solvents are a promising alternative although they are still in a 4 TRL [49]. They phase separate into two liquids, CO_2 lean and rich, when subjected to certain conditions [70]. This phenomenon implies less regeneration energy requirements, as well as lower reboiler temperatures compared to MEA processes [49]. Figure 5 shows a potential reduction of 15% in levelized cost of electricity (LCOE) when using biphasic solvents in CCS in a power plant. Next to this, precipitating solvents and improved conventional solvents reduce LCOE by 10% and 3%, respectively [49], [50].

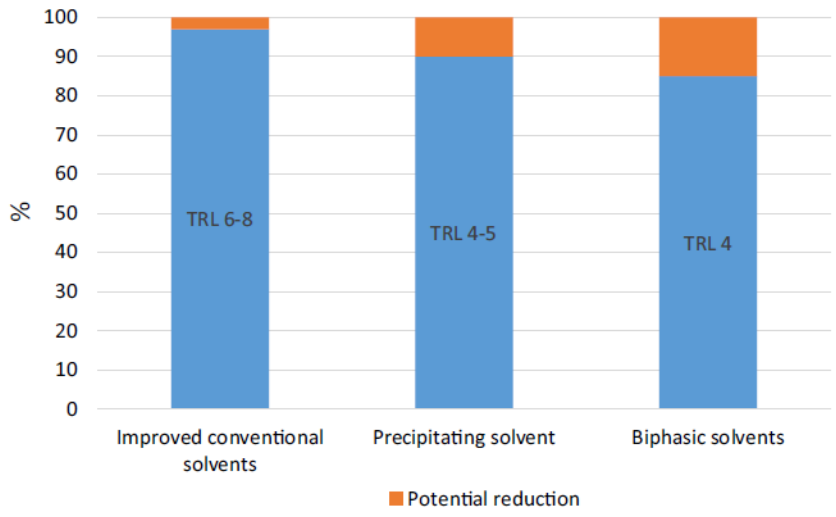

Figure 5. Levelized cost of electricity potential reduction from MEA based process installation [50]

When considering precipitating solvents, the main challenge lies on how to deal with precipitates in the absorber [72]. However, there exists a patented process employing amino acid salts based solvent whose capital and operating costs are about half of those related to a MEA based process [69].

Finally, in addition to considering new processes and solvents, combinations of these should also be placed under research, especially due to the general viscous nature of new solvents, which increases handling difficulty in common packed bed designs [49].

2.3.2.1.2-Amino-2-Methyl-1-Propanol (AMP) capturing system

AMP is a well-studied sterically hindered amine with high absorption capacity and low energy demand during regeneration [4], [73], [74]. Regarding new technological deployment, systems must present lower energy demands than available alternatives and if possible, to be able to substitute steam for low-value excess heat streams. One example of this kind of system is AMP in organic solvents, such as NMP or tryethylene glycol dimethyl ether (TEDGME) [74].

The mechanism for the CO_2 absorption and further reaction with AMP amine is presented in Reactions 1-4 [3]. Initially, CO_2 is dissolved (1) after which it reacts with AMP to form a zwitterion (2). This can further react with AMP and form a carbamate ion, $RNHCOO^-$, see Reaction 3, which can precipitate into carbamate solid, see Reaction 4 [74]. It is worth noting all these reactions are exothermic.

$$CO_2\ (g) \rightarrow CO_2\ (sol) \quad (1)$$

$$CO_2\ (sol) + RNH_2\ (sol) \rightarrow RNH_2^+\ COO^-\ (sol) \quad (2)$$

$$RNH_2^+\ COO^-\ (sol) + RNH_2\ (sol) \rightarrow RNH_3^+\ (sol) + RNHCOO^-\ (sol) \quad (3)$$

$$RNH_3^+\ (sol) + RNHCOO^-\ (sol) \rightarrow RNH_3RNHCOO\ (s) \quad (4)$$

In aqueous solutions, further reaction from carbamate into bicarbonate formation occurs [65], [75], [76]. If organic solvents are employed instead, this cannot occur. In this case, carbamate is the reaction end instead [4], [6], [75], [77]. Therefore, the solid carbamate compound is the one of importance in this work and its structure is presented in Figure 6.

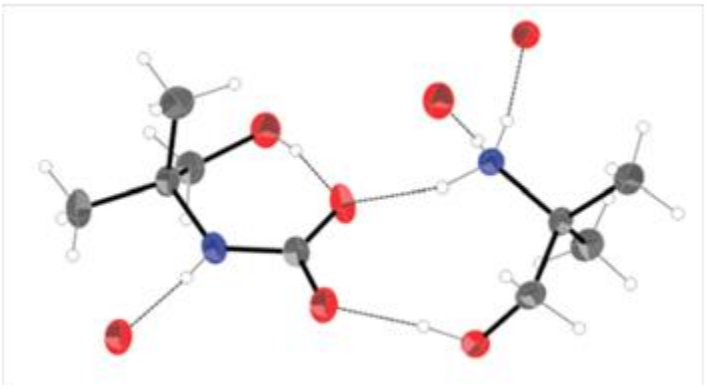

Figure 6. AMP Carbamate solid structure [78]

When and if precipitation occurs in the system depends on the solvent employed. When using AMP, the formation of this solid precipitate has been reported [4], [75], [79]. This aspect also

favours its use, especially when considering the nature of the compound obtained. The carbamate has an unstable nature, due to the amine's steric hindrance, and therefore, its regeneration is easier [76].

AMP based systems have been therefore gaining research interest lately [4], [77], [80]–[82]. The solid formation is an important characteristic of this new solvent system for CCS under study in this Master's thesis. Stoichiometry limits the amine loading in the system to 0.5 mole CO_2/mole amine. This value doubles when bicarbonate can be formed, i.e. in aqueous systems [74].

- Capture potential advantages

In general, the main advantage of a precipitating system is the possibility for separating the solid compound by, e.g., filtration, so less material is sent to regeneration [3]. Partly separating the stream sent to regeneration is an obvious advantage, less material needs to be heated up which will reduce the energy requirements in this step [74]. Also, smaller equipment size for this unit can be expected.

Considering AMP-NMP system, the possibility to regenerate the amine employing low-value excess heat with temperatures 70-90 °C has also been identified [74]. Desorption thus might become more cost-efficient, which in turn improves the overall process economy. The lower regeneration temperature presents extra advantages since it reduces the risk of hazardous amine emissions and the possible formation of degradation products [74].

This novel system also allows for pressurized CO_2 production, which can reduce further the energy requirement associated to CCS, through work compression reduction. In Figure 7, experimental results presented in [7] prove that it is possible to combine pressurized CO_2-rich stream production while still driving the regeneration within temperatures corresponding to low-value waste heat usage ranges. Furthermore, when comparing to MEA-based, the novel system reaches higher pressure in the stripper by a factor of approximately 3.

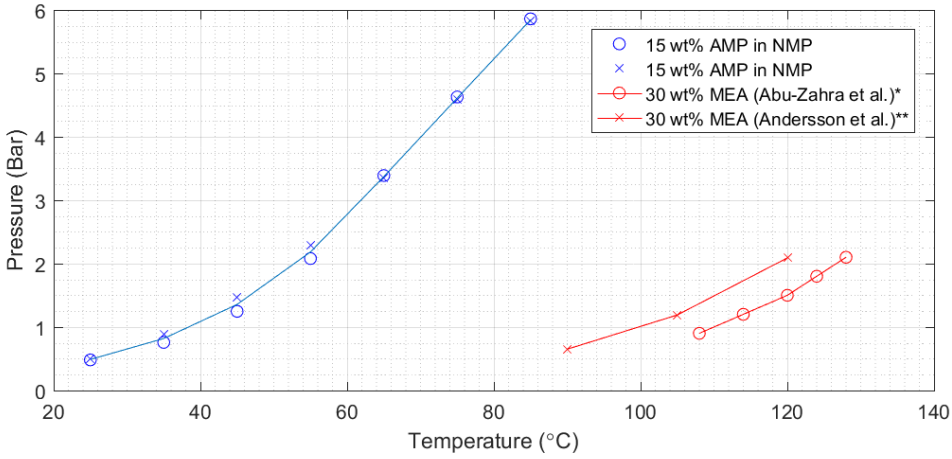

Figure 7. Comparison of CO_2 pressure for 15 w% AMP in NMP and 30%w aqueous MEA [7]

Thus, it is clear that this new solvent system represents an interest energetically efficient alternative to conventional systems. Additionally, it overcomes certain issues associated with

3. Method

The work in this Master thesis is split into several work-packages as shown in Figure 8. Three main sections can be differentiated: 1) AMP-NMP properties and process modelling, 2) sensitivity analysis and process optimization, and 3) case studies and comparison with benchmark aqueous MEA system. Each of these sections incorporated several tasks, which in some cases, were interrelated.

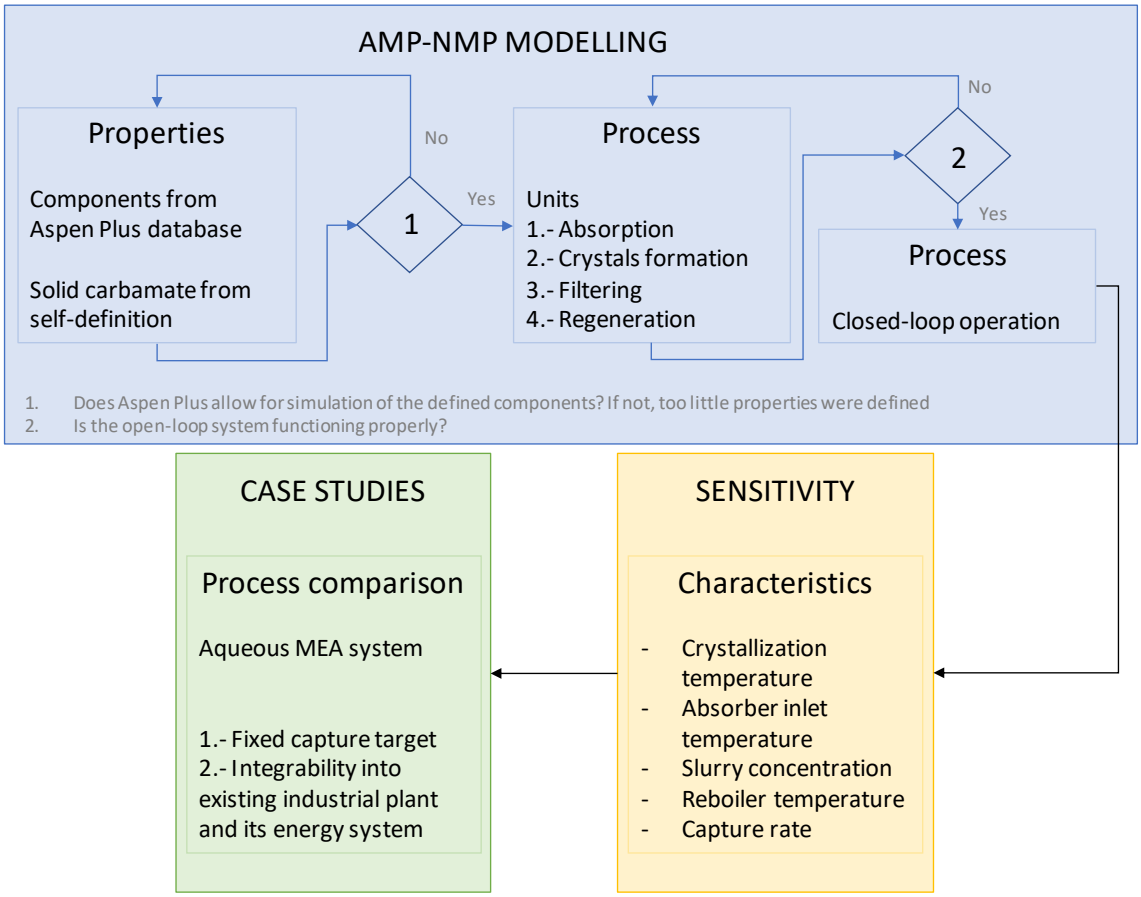

Figure 8. Work packages in this Master thesis

Below are separate chapters that provide detailed descriptions of the activities in each work package. The setup of the AMP-NMP property environment in Aspen Plus™ is explained in Section 4. Section 5 covers all the aspects related to process modelling of the novel AMP-NMP system. More specifically, 5.1 details how the process is setup in Aspen Plus™; in Section 5.2, the process parameters towards key performance indicators is analysed and in Section 5.3, an industrial case study on CO_2 capture from a Swedish oil refinery is conducted with emphasise on the comparison between aqueous MEA and the novel AMP-NMP system.

4. Property environment

The first step to model or simulate a certain system is to define the properties associated to it. In this section, the different choices regarding calculation methods, reference states for the components and property inputs for some of them are presented.

There are components in the AMP carbamate precipitating organic system for which not all required properties for a proper definition are available in databases. More specifically, the solid compound and the zwitterion are not directly available in Aspen Plus™. Therefore, their properties were estimated in those cases where no information or experimental data was encountered. The minimum information required to include a component in the software can be found in Appendix 1. It is important to highlight that estimated properties affect the overall properties in mixtures.

4.1. Reference and property method in Aspen Plus

The choice of property method in Aspen Plus is affected by the type of components present in the CCS system which are gases, liquids, ions and solids.

Since ions are present, a reference state must be chosen for them between symmetric and unsymmetric. For the former, either equilibrium constants must be directly provided or data for its regression. Activity coefficients are based on those for pure fused salts and water does not have to be defined as a component. For the unsymmetric definition, which is the one employed in this work, constants are calculated directly from the reference state Gibbs free energies of the components involved. Activity coefficients are instead based on infinite dilution in pure water, which must be defined as a component and be present in the system [83]. This means the system is treated as if it was an aqueous one when, in reality, it is organic based.

The presence of ions also influences the property method to be used, either “ELECNRTL” or “ENRTL-RK” should be selected [83]. The main differences are related to how mixture properties are calculated. In fact, their use in systems with a single electrolyte delivers identical results. However, when there are mixed electrolytes, “ENRTL-RK” applies mixing rules to retrieve pairwise interaction parameters and these are not used for Gibbs free energy calculations. This method creates a single thermodynamic framework in which activity coefficients, Gibbs free energy and enthalpy are calculated, whereas “ELECNRTL” employs separate models [83]. In this master thesis, “ENRTL-RK” was selected as method for the process simulations. The motivation for its selection can be found in Appendix 2. In addition to this, with regard to the presence of a zwitterion, both options apply unsymmetric Electrolyte NRTL method for handling it [83].

4.2. Zwitterion

When selecting the reactions taking place in the system one must be careful since increasing the number of reactions implemented increases the complexity in the system which may end up in some cases with non-converging solutions [91]. In the present system, this is mainly related to the presence of a zwitterion.

The zwitterion is not going to be a compound significantly present, rather a fast reacting intermediate, with at least 10^{18} times smaller flow than AMP and its carbamate ions (Appendix

3). Due to its low concentration, removing the zwitterion from the components present in the system is considered valid. Consequently, Reactions 2 and 3 were combined into Reaction 5 when implementing the chemistry and reactions in the process simulation.

$$CO_2\ (sol) + 2\ RNH_2\ (sol) \rightarrow RNH_3^+\ (sol) + RNHCOO^-\ (sol) \quad (5)$$

4.3. Solid

Although Aspen Plus™ was set to "Estimate all missing parameters", some key values could not be obtained through group contribution estimation in this software, presented in Table 3. This was recognized from the fact that chemical reactions could not proceed due to missing parameters.

Table 3. Required parameters not estimated

Component	Missing property	Method
Solid	Gibbs energy of formation	Solubility data in [80], [84]*
Solid	Heat of solid formation	Heat of absorption data, [85]**
Solid	Solid molar volume	Calculated from density in [78]
Solid	Heat capacity	Estimated through Cranium™, [86]

*Unpublished data by Sanku, M. and Svensson, H. from Lund University
**Unpublished data by Karlsson, H. and Svensson, H. from Lund University

In Aspen Plus™, all these parameters can only be estimated through contribution groups via Mostafa method which is only applicable to inorganic compounds [87]. Therefore, experimental data or other estimation tools had to be employed for these solid properties determination.

4.3.1. Solubility - Gibbs energy of formation

Gibbs energy of formation allows Aspen Plus to determine the extent of a certain chemical reaction. Normally, equilibrium constants are directly calculated by Aspen Plus™ from these parameters when selecting the unsymmetric reference state. However, they can also be accessed and turned into user defined parameters. This path was followed to handle the solid AMP carbamate formation. More specifically, the alternative was to implement the solubility function, which also provides the extent of the precipitation reaction. The data is provided in the Properties definition, under Chemistry.

Therefore, the solubility data from experimental measurements in [80] was regressed to fit models based on coefficient combinations from Equation 1, which could be later implemented in the simulation in Aspen Plus™.

$$\ln K_{eq} = A + \frac{B}{T} + C\ln(T) + D \cdot T + E \cdot (P - P_{ref})/P_{ref} \quad (1)$$

Since the data available was obtained solely as a function of temperature, the term regarding pressure was omitted in the regression. Temperature is expressed in Kelvin and the solubility

equilibrium constant in mole fraction. Several scenarios, including all, pairs or single coefficients (A-D) were considered to obtain the best fit (Appendix 4).

Data fitting to Equation 1, considering parameters A-C-D, for the solubility data is presented in Figure 9. This is the case with higher applicable fitting R-squared (0.954). Confidence intervals - with 95% confidence - were calculated for this case and found to lie within reasonable margins; results are shown in Table 4**.**

Table 4. Model parameters regression for Equation 1 application

Parameter	Lower bound	Value	Upper bound
A	-1859	-1066	-273.9
C	52.06	217.1	382.2
D	-1.091	-0.5924	-0.09386

The solubility curve implemented in Aspen Plus™ is presented in Equation 2.

$$\ln K_{eq} = -1066 + 217.1 \cdot \ln(T) - 0.5924 \cdot T \quad (2)$$

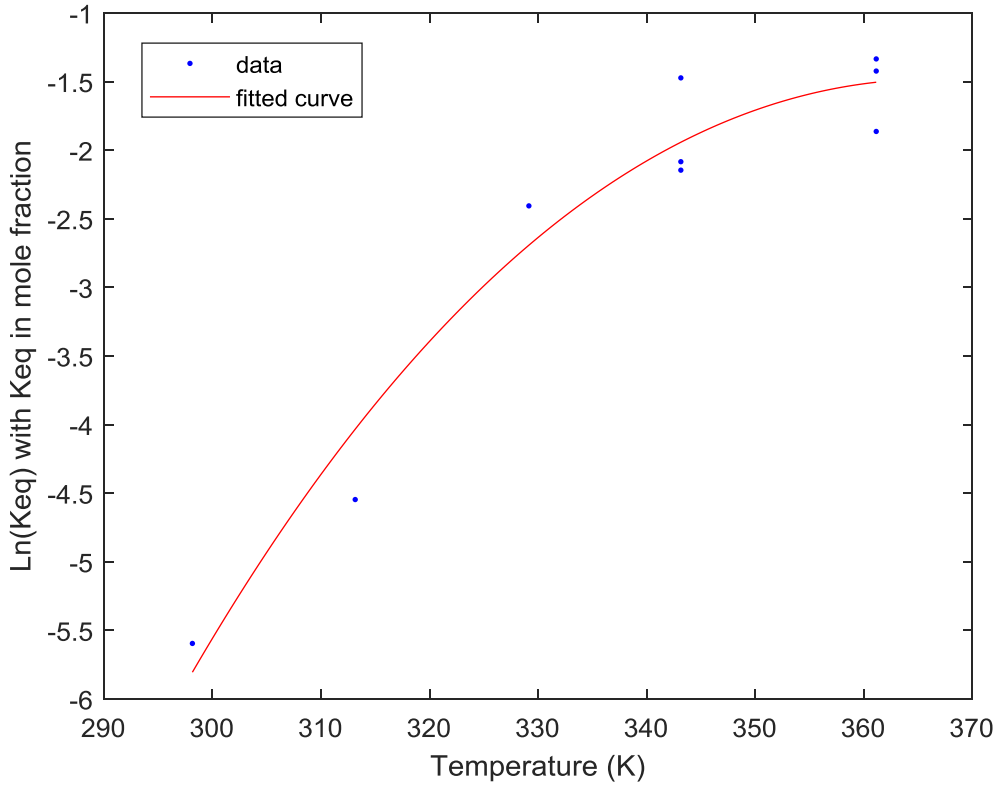

Figure 9. Solubility data fit to the chemical equilibrium equation

4.3.2. Heat of absorption – Solid heat of formation

The heat of absorption covers all reactions occurring parallel in the system (Reactions 1-4 in 2.3.2.1), when considering experimental measurements at Lund University set up. Published data regarding heat of absorption can be found in [88], along with the set up description. This Master's thesis employed additional data in [85]. These measurements obtain the heat

released when CO_2 is injected in a system containing certain amount of solution, in which CO_2 is absorbed from the gas phase and reacts further.

The parameter required in Aspen Plus™ is the solid heat of formation, which cannot be directly obtained from experimentally measured data. In fact, to be able to directly obtain it from experiments, the only reaction in the tested system should be the solid forming from its precursors, which does not occur. Therefore, a different approach had to be followed for its estimation, which is described in Appendix 5. It is important to highlight that this is a first approach for determining these properties for the solid formation. To be able to understand the limitations and the overall effect of the assumptions in this process, the solid heat of formation was included as a parameter to be tested in the process simulations, see Section 6.1.

4.3.3. Density – Solid molar volume

To determine the volume a certain mass of solid occupies, Aspen Plus™ requires as input parameter the solid molar volume, *v*. It was calculated from the density value in [78], according to Equation 3.

$$v = \frac{1}{1{,}214\frac{g}{cm^3}\cdot 10^6\frac{cm^3}{m^3}\cdot\frac{1\ mol}{222{,}28\ g}\cdot\frac{1\ kmol}{10^3\ mol}} = 0{,}1831\frac{m^3}{kmol} \quad (3)$$

Molecular weight value was extracted from Aspen Plus™.

4.3.4. Property estimation – Solid heat capacity

For solid heat capacity, no source of experimental data has been found nor any calculation route. Therefore, this parameter was estimated with a different software, Cranium™, [86]. The solid structure was provided to generate property estimations of several properties through different methods. Detailed information can be found in Appendix 6.

4.4. Limitations

The system under study constitutes a novel technique, not as much information regarding neither component properties nor its chemistry is available as for other systems, such as aqueous MEA, which have been researched into for longer time. This is itself a limitation, especially when considering further process scale up.

Considering further limitations in the modelling of the new solvent, a closer description of the most significant is included.

- Aspen Plus™

The software employed for the process simulation, as explained before (see 4.1), presents two alternatives to handle chemistry involving ions. The fact that the reference state was chosen as unsymmetric is an approximation limiting the system to perform closer to reality. The software considers the ions to be in an aqueous solution, even though most of the solvent in the simulations is NMP. This aspect has an effect since mass transfer is considered in the simulations and it has shown to be faster for amines in organic solutions. In addition to this, since this is the step limiting the overall chemistry, organic based solutions are expected to perform better in this aspect, which is not included with the current system definition [89].

Since kinetics were not included in the scope of this master thesis work, the fact that the system was defined as unsymmetric was not expected to affect the results significantly. However, this is certainly an aspect to consider for further model development. In order to select the proper reference state for the ions, which is symmetric, great efforts should be devoted to experimental data collection so all separate reactions could be defined with its separate equilibrium constants. Most likely, these would need to be evaluated at different points in the temperature range within which the model would operate. Aspen Plus™ software includes property regression for user input experimental data. If this includes the chemistry equilibrium constants should be checked.

- Solubility

There are two major routes in which the solid formation, dictated by the input for the solubility, is limited: the experimental set up and the data fitting accuracy.

When it comes to the fitting, the accuracy of the parameters in the model is not good enough when considering all possible terms of Equation 1 (Appendix 4). Moreover, this complete model had to be turned down due to the too extensive confidence limits, including both positive and negative ranges. This could be improved with more experimental data in the considered temperature range, between 25 and 90°C, so that the model can become more reliable.

However, even though further experimental data would improve the fitting, there is a major limitation regarding the experimental set up. Solubility measurements, as described in [79] were performed in an enclosed recipient. Initially, a known amount of solid was introduced. After which, solution 25%w AMP in NMP was added until crystals were no longer detected. The fact that there was gaseous phase in the recipient means that it was possible for reactions to further proceed. Solid was not only dissolving into ions. Also, AMP and dissolved CO_2 in the solvent and even release of this into the gaseous phase was occurring. Therefore, considering that only the ion formation was significant in these measurements was an approximation. This means the solubility chemistry input in the software was under-predicting solid precipitate formation. More solid can be dissolved in the measurements than it would actually do if only the ion formation occurred, as the fact that the ions form other compounds pushes equilibrium towards dissolved species. An approach to be able to identify solubility itself could be to perform liquid speciation, necessary information for more accurate system representation, as previously suggested in [80].

- Heat of absorption

The system chemistry also influenced the experimental measurements for the heat of absorption. This means the separate contribution from Reactions 1-4 could, again, not be determined. The uncertainty related to the speciation added to the impossibility of determining how much solid was produced limited the separation into individual contributions of Reactions 1-4 to the heat being released. Regarding this property, it is of greater importance to be able to obtain quantitative data for the solid formation than for the speciation. Moreover, the assumptions presented in 4.3.2 lead to an optimistic value of the heat associated to the crystal production. Lesser solid formation than the total CO_2 absorbed can be

expected, which in turn would mean that the heat associated to the solid formation would be higher. The less solid being formed, the more heat would be assigned to each precipitating mole since the heat measured in this experimental point is a non-changing value. To consider this effect, it was determined to vary the amount of solid precipitating. Therefore, the underlying property, the heat of solid formation, was considered a parameter.

In addition to this, it must be remarked that the property input required in Aspen Plus™ cannot be directly calculated, since the solid is not forming from its precursors in the system, and instead an iterative approach was conducted to check the heat calculated in the crystallizer per mole crystal. This represents another source of discrepancies. The experimental set up and software crystallizer do not operate at the same temperature. The difference was allowed as attempt to mimic the sudden precipitation in the experimental set up. Since the precipitation occurred in the open-loop simulation at 33 °C, the stream is cooled down in the heat exchanger to 34 °C and then, enters the crystallizer block set to operate at 33 °C.

- Heat capacity

Parameter estimation with the actual solid compound was not retrieving all the desired parameters since the solid structure could not be split into recognizable groups for some of the available estimating methods. Since the Cranium™ version employed is the basic demonstration, it was found out that certain estimating techniques are not included. This means it would be possible to retrieve more accurate estimations for this property. However, it is not as critical to the results as the other parameters. So far, the current estimation for the solid heat capacity was enough to complete solid definition requirements according to Table 3.

5. Process modelling

The capturing process for the novel system AMP in NMP was modelled in a closed-loop simulation. Reaction kinetics are not implemented - as data for AMP-NMP is not available. The previously developed model for MEA, as presented in [90], was adjusted to set common ground to allow fair comparison. Processes, as well as their commonalities and differences are detailed in the following subsections. In addition to this, the setup for a case study comparing both solvent systems for CO_2 capture from a Swedish oil refinery is presented.

5.1. Simulation environment

The 30 wt% MEA-based absorption process model in Aspen Plus™ is adapted from [90] and the novel 25 wt% AMP in NMP system is developed from [91].

5.1.1. Organic AMP-based model

A process flowsheet of AMP in organic NMP solution is presented in Figure 10. Note that the process units in red are only included in the Aspen Plus model and are not suggested for a real process. A certain flue gas is treated in the absorber, which is a packed column. The CO_2 lean flue gas leaves the absorber at the top and it is sent to the stack. The CO_2-rich solvent stream is cooled down and introduced into a crystallization block where the solid is formed according to the regressed solubility curve, see 4.3.1. The solution is partly separated from the solid giving a carbon (crystal) rich stream that is sent to regeneration. There is a cross-flow heat exchanger to recover heat from the hot regenerated solvent. For the regeneration, the solvent is stripped in a packed column. The regenerated lean solvent goes through the cross-flow heat exchanger, after which it is mixed with the solvent previously separated from the solid rich stream. Impurities in the system are purged and a solvent make-up is added to balance the solvent system. A heat exchanger is included prior to the solvent recycle to the absorber to ensure constant inlet temperature.

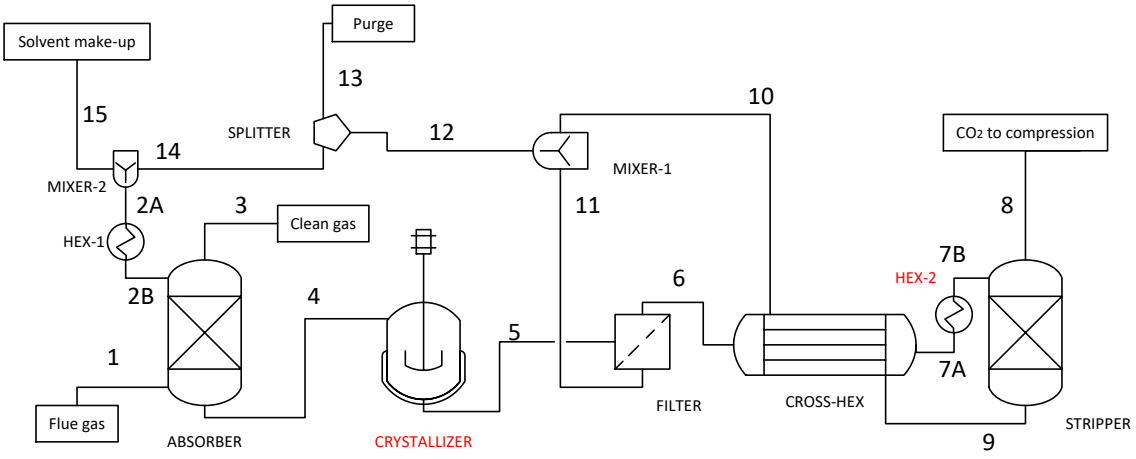

Figure 10. Organic AMP process flowsheet (names in red represent equipment included only for modelling)

Chemical reactions in the absorber are defined to be in equilibrium. Compared to the process model presented in [91], the regeneration section has been modified, i.e. a cross-flow heat exchanger and the solvent split were included. In addition to this, no pumps have been included. These were considered to have the major impact in cost estimations, which are not part of the scope of this Master's thesis. However, its inclusion would have been important

regarding the analysis of the compressed CO_2 production, which was not included either in this analysis. Mapping the effect of the regeneration temperatures could be accomplished without the pressurized CO_2 stream. The method employed for the calculations in the simulation is kept constant, “ENRTL-RK”.

Now, specifically considering the different units, sections and process conditions, certain features are highlighted.

- Absorption

The absorber block was defined as rate-based model with chemical equilibrium, i.e. including mass transfer. The column is modelled with 30 stages column and a packed height of 20 m, using 250Y standard Mellapak. The diameter was set to limit flooding to a maximum of 78%.

Aspen Plus™ does not allow to perform rate-based calculations with stage-by-stage solid crystals in the absorber. This is closely related to the presence of solid crystals in the absorber inlet. Thus, a heat exchanger, HEX-1 in Figure 10, was placed upstream of the liquid inlet to ensure this condition was fulfilled.

- Crystallization

The crystallizer was modelled to determine the solid formation through the chemistry definition in the property environment, i.e. the experimental solubility, see 4.3.1. In the closed-loop process, solids were found at a lower temperature due to the increased ionic concentration, 30 °C vs 33 °C in open-loop, see 4.3.2.

This feature is exclusive to precipitating systems and therefore, there is nothing comparable in the MEA-based process.

- Filter

This unit partly separates the liquid and solid phases in stream 5 into two streams: retained solid - stream 6 - and liquid filtrate - stream 11. All streams numbers refer to those defined in Figure 10. The filter was set to separate 99% solids, i.e. 99% of the moles of the solid in stream 5 go into stream 6. Additionally, the amount of liquid in stream 6 was defined through a slurry concentration target. The amount of liquid in the solid retained is calculated via a design specification that sets the solid concentration to a certain molar fraction, 20% for the base case, see Table 7 in section 5.2.2.

- Cross-flow heat exchanger

In this unit, the retained solid stream is heated by the regenerated stream exiting the reboiler in the stripper. The hot side inlet is therefore the reboiler temperature and the cold side inlet, the temperature in the filter, equal to that set in the crystallizer. The unit is defined to recover as much heat as possible by setting a temperature difference between cold inlet and hot outlet of 10K.

- Regeneration

The regeneration was modelled with a stripper set in rate-based, i.e. including mass transfer. It is a packed column, modelled with 20 stages and 15 m packed height with 250Y standard Mellapak. The diameter was set to limit flooding to a maximum of 80%.

As in the absorber, a heat exchanger was placed before entering this unit to ensure no solids were entering. The temperature for the regeneration is selected so no solids remained in solution. Based on the experimental data presented in [7], the recommended temperature of 90 °C was set in the base case to avoid the possibility of encountering secondary precipitation, even though this phenomenon could not occur in the modelled process.

5.1.2. Limitations

In the AMP-NMP system model, there are two main sources for limitations: data availability and the software itself.

- Data availability

When moving from properties to simulation environment, the speed and actual extent of the reactions considered can be expressed by implementing the system kinetics. However, this information was not available for the AMP system. It is not clear how much this affects the overall process performance since either reactions or mass transfer could be limiting the absorption. If chemical reactions were faster than mass transfer, the effect would be practically inexistent. However, if they were not, the new solvent system would be over-predicting the actual capture. Since MEA system kinetics were available, the effect of kinetics on this system was evaluated and analysed, see Appendix 7.

- Software

Aspen Plus™ presented several limitations when simulating AMP-NMP system. As it was previously mentioned, it was not possible to perform rate-based calculations when crystals were present in the absorber inlet. This limits the possibility for cooling in the inlet and to increase process performance. It is also a breach from reality as crystals were expected to start to form inside the absorber. Additionally, this reflects in the regeneration where the heat for regeneration needs to be split into the stripper reboiler and a pre-column heat exchanger to prevent solids from entering this Rad-Frac block. In this sense, alternative definitions could be considered, such as selecting different sort of component, e.g. non-conventional, though that may limit the chemistry definition, i.e. the precipitation.

5.2. NMP-AMP process optimization

Several parameters are considered regarding the process modelling performance in both the property and simulation environments in Aspen Plus™. The optimization is carried out employed as flue gas a blast furnace gas, with the gas conditions and composition defined in Table 5. Note the pressure above atmosphere and the high CO_2 concentration.

Table 5. Blast furnace gas definition, [92]

Flow conditions			**Composition (mol%)**					
Temperature (°C)	**Pressure (kPa)**	**Flow (kNm^3/h)**	**CO_2**	**N_2**	**O_2**	**H_2O**	**CO**	**H_2**
29	181.3	352.41	24.6	49.7	0.0	2.2	20.4	3.2

5.2.1. Solid properties sensitivity

To analyse how the assumption of total crystal formation underlying in the calculations for the solid heat of formation, see section 4.3.2 and Appendix 5, impacts the overall process requirements a study was carried out considering the cases shown in Table 6. The reader is referred to Appendix 5 for a detailed explanation on what was done and how. The third column stating the heat per solid formed in the simulation is the amount of heat released in the crystallizer unit whereas the forth, the estimated solid heat of formation is the parameter used as input in the property environment in Aspen Plus™. The key performance indicator considered in this case is the specific heat demand of the process, as it is directly related to the solid, its concentration into the retained solid and therefore, the energy required for it to go back into free amine in the liquid and gaseous CO_2.

Table 6. Solid heat of formation sensitivity analysis

Case	**Assumed solid precipitate (mol CO_2 absorber to mol solid crystal)**	**Heat per solid formed in the simulation (kJ/mol solid)**	**Estimated solid heat of formation (kJ/mol solid)**
1	100%	121.343	$-1.393 \cdot 10^3$
2	90%	134.825	$-1.548 \cdot 10^3$
3	80%	151.678	$-1.741 \cdot 10^3$
4	70%	173.347	$-1.990 \cdot 10^3$
5	60%	202.238	$-2.322 \cdot 10^3$
6	50%	242.685	$-2.786 \cdot 10^3$

5.2.2. Process characterization

The effect of certain parameters on the process conditions in the developed AMP-NMP model and the potential for carbon capture was analysed by focusing on key performance indicators. The data collection for analysis included liquid to gas (L/G) ratios, CO_2 loadings throughout the system and specific heat demands, among others.

Variables are considered from a base case and varied. Base case conditions summary is shown in Table 7. These variables were controlled through design specifications, when it was not possible to select them directly as block or stream defined.

Table 7. Process conditions definition and manipulated variables

Parameter varied	Type	Base case	Sensitivity range	Units	Definition	Manipulated variable
Crystallization temperature	Model	25	20-30	°C	Block	-
Absorption inlet temperature	Process variable	35	30-40	°C	Block	-
Solid concentration	Design parameter	20	10-30	%	Design	Liquid to solid outlet
Regeneration temperature	Process variable	90	70*-90	°C	Design	Reboiler heat load
Capture rate**	Process variable	90	50-90	%	Design	Liquid circulation

*Instead of 70 °C as regeneration temperature, 71 °C had to be set due to constraints in solid modelling

**All cases set the liquid to gas ratio to achieve a 90% capture. When the capture rate is varied, the design point for this parameter is varied accordingly.

From Table 7, a clarification needs to be included for the capture rate. The target in the design specification is the outlet CO_2 set as component flow. The manipulated variable is the liquid circulation set in the absorber inlet, which is equivalent to varying the L/G since the flue gas inlet is fixed. The reason for this setting is that one of the advantages of only aiming for partial capture is that the partial pressure of the CO_2 in the outlet would be higher and therefore, separation easier to achieve.

When varying a single parameter in the model, the entire process is affected since it is run in closed-loop mode. Normally, the relation between the closely related variables, i.e. those related or result of a block, is more pronounced. However, the filter in this system acts as a decoupling agent. Therefore, it is expected that variables related to the absorption part present major impact between them and similarly, between those in the regeneration part. Obviously, there is also a relation between sections as, e.g. the lean loading exiting the regeneration section is an input to the absorption one and inversely, the rich loading constitutes an input to the regeneration.

5.3. Aqueous MEA and organic AMP systems comparison

The basis for comparison between organic AMP and benchmark process employing aqueous MEA as solvent in different scenarios is presented. Key parameters were identified for this purpose and are summarized in Table 8.

Table 8. Key parameters for process comparison

Parameter	Block/Stream	Units
Lean loading	Liquid absorber inlet	(mol/mol)
Rich loading	Liquid absorber outlet	(mol/mol)
Liquid to gas ratio, L/G	Absorber	(mol/mol)
Mass transfer area	Absorber	m^2
Specific heat demand	Regeneration	MJ/kg CO_2
Specific cooling demand	Coolers, crystallizer	MJ/kg CO_2
Solvent slip - Clean gas	Absorber	mole frac.
Amine slip - Clean gas	Absorber	mole frac.
CO_2 purity	Stripper	mole frac.
Solvent slip - CO_2-rich	Stripper	mole frac.
Amine slip - CO_2-rich	Stripper	mole frac.

5.3.1. Aqueous MEA-based model

The model in [90] included certain process configuration improvements, such as a split flow and an absorption inter-stage cooling. The process adjustment included their removal from the simulation environment so that MEA process became simpler and closer to the basic configuration, see Figure 3. Additionally, chemical reactions were originally defined through kinetic reactions. However, since these were not available for AMP, MEA reactions were re-defined to be in equilibrium. Finally, it is worth noting that the simulation for MEA is run in a different property method, “ELECNRTL”.

5.3.2. Performance of 90% capture

It was determined that processes performance should not be limited by any of the factors in Table 8 as that could lead to favouring one or another. Both processes were set to capture 90% inlet CO_2 separately within certain feasibility conditions, e.g. regeneration temperatures were set below the amines degradation temperatures. It was considered that setting the comparison out in this way represented an un-biased approach. In this case, for both processes, also the gas defined in Table 5 was employed as flue gas inlet.

5.3.3. Industrial case - Swedish oil refinery

One of the major drawbacks for CCS deployment is the cost to regenerate the solvent. Thereby, possibilities to integrate this part with the specific site energy systems are of great importance. In this sense, available low-value waste heat is considered as potential heat source for the CCS plant.

For such comparison, both processes were considered for integration in a Swedish oil refinery. Information regarding oil refinery conditions is extracted from prior publications. First, available stacks that could be targeted for carbon capture are presented in Table 9.

Table 9. Characteristics of the flue gases at the different stacks of the refinery, composition in mol%, [63][93]

Stack no./source	CO_2	N_2	O_2	H_2O	Temperature (°C)	Mass flow (Mt/yr)
Stack 1 - heaters	8	73	4	15	160	4.9
Stack 2 - heaters	9	72	4	15	180	3.0
Stack 3 - FCC	14	70	1	15	270	1.0
Stack 4 - SMR, heater	24	59	2	15	170	1.8
Stack 5 - heaters	8	74	3	15	130	0.5

Regarding available heat, since the solvent regeneration temperature in both systems differ, also different amounts of low-value waste heat are available for the capture unit. Two cases were initially considered: 1) An actual representation of the refinery, accomplished through the actual cooling loading curve (ACLC) and 2) A retrofitted energy network in a maximum energy recovery (MER) heat exchanger network. Available heat was obtained with a 20K temperature difference to the one that would be set in the regeneration unit, to allow 10K minimum temperature difference with each side of the circulating fluid collecting this heat. In Figure 11, this is presented for the two temperature levels considered for the organic AMP system, 90 and 75 °C. To consider these alternatives was derived from the process sensitivity, see sections 5.2.2 and 6.2.4.

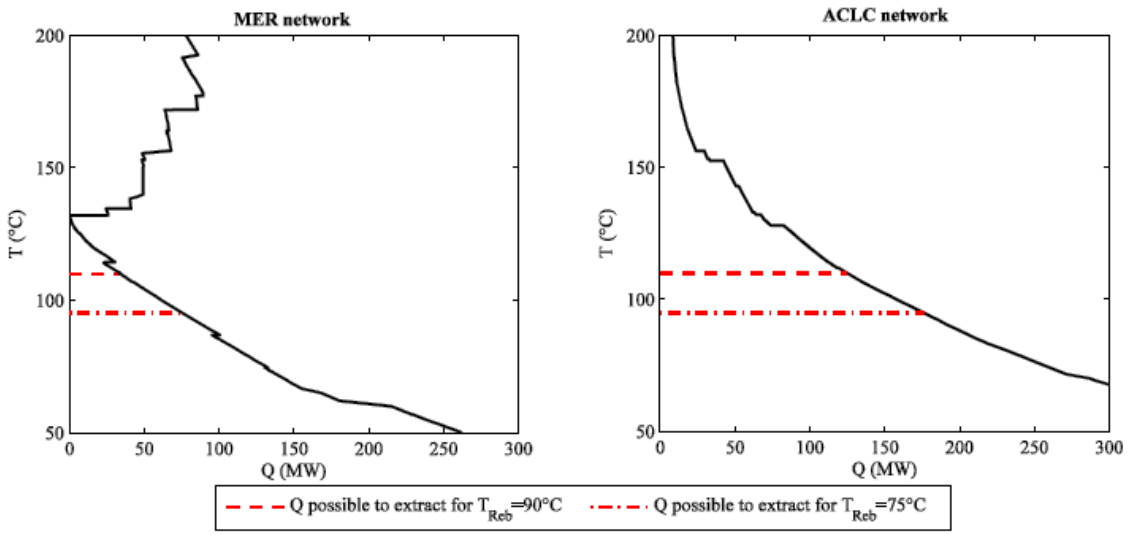

Figure 11. T/Q diagrams of a maximum energy recovery (MER) heat exchanger network and the current cooling utility network (ACLC), [1]

From the information available, several industrial cases could be built. This Master's thesis targets Stack 4, the flue gas from steam methane reforming, due to the high CO_2 concentration and sufficient flow. Regarding excess heat, it was considered that it was possible to employ the actual cooling load curve, as it is the best representation of the current refinery state operated in practice. This means much more heat was available for the integration. Additionally, the

heat available in both cases to supply energy to MEA case must be checked since the objective is to compare its performance to the novel AMP system. In this case, the temperature for regeneration is 120 °C and to allow for the same minimum temperature difference, heat at 140 °C is extracted. For MER network, it is possible to see the pinch point, the one where the graph touches the Y-axis, has come down 131.7 °C, which means there is no heat available to power the regeneration in the MEA process. Most likely, the optimization of the MER did not consider CCS. However, it reflects those cases where AMP-NMP CCS process could be considered whereas not one employing aqueous MEA, given that the regeneration is powered only with excess heat. The available low-value excess heat to power regeneration in each case is summarized in Table 10.

Table 10. Available low-value waste heat for partial carbon capture in each process

	AMP process	AMP process	MEA process	Units
Reboiler temperature	75	90	120	°C
ACLC network case	175.9	125.4	54.5	MW
MER network case	76.2	34.2	-	MW

6. Results and discussion

The results obtained from the process simulations are presented as following. At first, the behaviour of the chosen AMP in NMP property environment is evaluated towards a critical property parameter concerning solid formation. Subsequently, the NMP-AMP process model is characterized in its performance in dependence of important process variables. Then, this new process is compared to benchmark aqueous MEA. The focus is placed around energy usage, capturing potential and solvent circulation, as these impact the overall process efficiency. Finally, their performance in an industrial case powering the regeneration with low-value waste heat is compared.

6.1. NMP-AMP property environment

The relation to the estimated heat of solid formation is presented in Figure 12. The linear dependency between the specific reboiler heat demand and the estimated solid enthalpy of formation, see Appendix 5, is expected. The amount of solid precipitate in the process is constant. Therefore, when the heat of solid formation increases - notice the negative axis referring to released heat in its formation, which has then to be provided in the regeneration -, the heat demand is proportionally higher.

Figure 12 also shows the relationship between the specific heat demand and the amount of solid precipitate. This parameter represents how much of the CO_2 absorbed in the system goes into the solid crystal formation. The specific reboiler heat demand increases if less CO_2 is assumed to form solid precipitate. Moving from 100% to 50% precipitation results in an increase by a factor of 5 showing how critical the assessment of solid heat of formation is for the process performance.

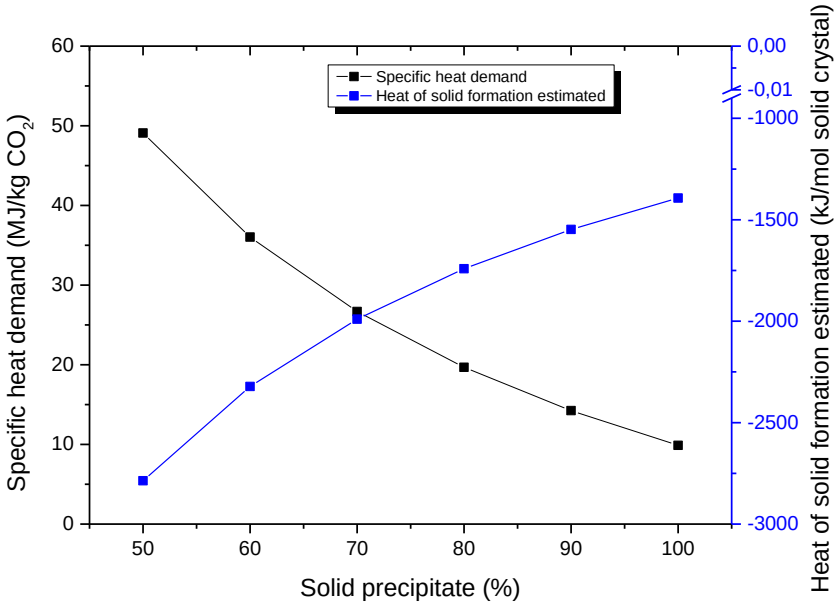

Figure 12. Specific heat demand and heat of solid formation for the estimated solid precipitates

Considering the experimental results, the specific heat demand was expected to be 14.4 MJ/kg CO_2 [94]. The model estimates the heat demand to be in the same order of magnitude at solid precipitation rates close to 90%, where it is 14.2 MJ/kg CO_2. However, 100% CO_2 solid

precipitation with a base value for the specific heat demand of 9.89 MJ/kg CO_2 is used in the process model analyses. Note that the property parameter that is defined in Aspen Plus is the heat of solid carbamate formation estimated to be -1390 kJ/mol solid crystal. This selection was due to the likelihood for energy losses related to lab scale experiments and since this set-up did not include a cross-flow heat exchanger, which increases energy efficiency.

6.2. NMP-AMP process sensitivity

The most relevant variable interactions for the AMP-NMP system are given in Table 7. Common for all parameters considered in the sensitivity analysis is that rich loadings are lower than the measured variables in the experimental studies; see [95]. In some cases, differences may be related to numerical differences in Aspen Plus™ itself since the L/G ratio is set through a design specification directly modifying the liquid inlet to the absorber to meet the design target of 90% capture for all tested sensitivities.

6.2.1. Crystallization temperature

As temperature is increased higher L/G and lower regeneration requirements, i.e. less material flow - overall amount in stream 6 - is regenerated, are observed to meet the 90% capture target. Since the regenerated amount decreases with increasing crystallizer temperature, the system needs higher solvent circulation to achieve the 90% capture target.

In Figure 13, the CO_2 loadings throughout the system are presented. As a reminder, lean, rich, solid concentrated and regenerated correspond in Figure 10 to stream numbers 2B, 4, 6 and 9, respectively. Rich and solid concentrated follow a similar trend, with increasing crystallization temperature their loading is increased. This trend is even more distinct in the case of the lean loading. Regenerated stream loading remains practically constant for the applied crystallization temperature range.

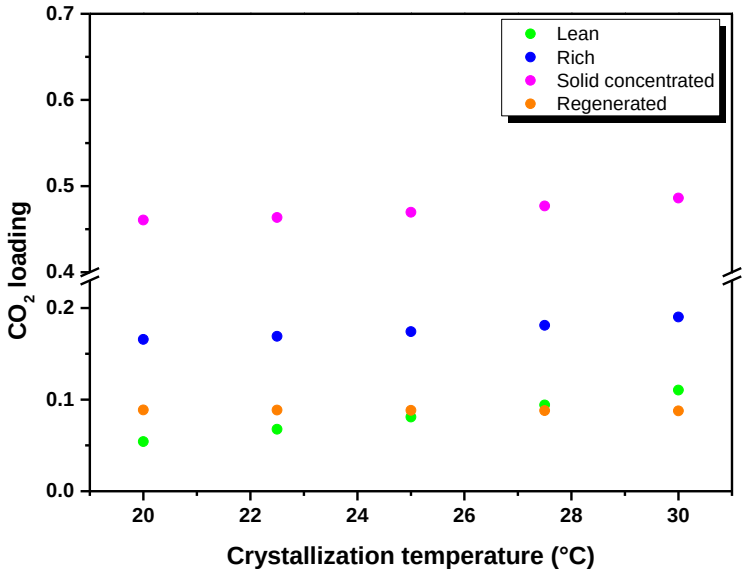

Figure 13. CO_2 loading sensitivity to crystallization temperatures

The process parameter that is affected the largest by the crystallization temperature is the solid concentrated loading. Its increase in the retained solid stream with lower crystallization temperature is analysed. The common 20% solid molar content provides same CO_2 loading.

Thereby, the difference lies in the liquid, in its higher ionic concentrations. This is explained by the crystallization where the temperature decrease pushes the equilibrium towards solid formation. This results in the depletion of stream 4, see Figure 10, from ions. Stream 4 and 5, before and after crystallization, have the same CO_2 loading. Their difference is in which species the CO_2 is retained. The more solid is formed, the more ions are transformed. This results in lower CO_2 loadings in the liquid phase in stream 5 and stream 11, the liquid filtrate.

Therefore, the proportional amount of organic liquid phase that is separated in the retained solids stream in the filter plays a major role. Those with higher ionic concentration - those with lower crystallization temperature - present higher loadings and result in higher loadings for the solid concentrated - or solid retained.

The loading in the regenerated stream remains basically constant as the crystallization temperature is varied reflecting that these parameters are not significantly correlated. The changes observed in the lean stream derive mainly from the mixing of the liquid filtrate and the regenerated stream. It presents a significant increase with increased crystallization temperature which is basically related to the influence the liquid filtrate has. This is explained by the contribution of two factors.

1) The amount of material in the retained solid stream. As the crystallization temperature is increased, the ratio between retained solid stream/liquid filtrate decreases. Therefore, when the streams are mixed after regeneration, the liquid filtrate influences more the outcome of the mixture due to its greater material content.
2) The loading of the liquid filtrate, see previous explanation on the ionic depletion.

Both parameters influence the resulting lean loading. Finally, this stream is the one entering the absorber, which influences the L/G required to accomplish the 90% capturing target and the resulting rich loading in the liquid stream exiting this unit.

The specific heat demand in the process for the considered crystallization temperatures is presented in Figure 14. There seems to be a maximum specific heat between 22.5 and 25 °C. This can be related to the heat required in the heat exchanger removing solids prior to stripping, HEX-2 in Figure 10, and, in turn, to the recovery accomplished in the cross-flow heat exchanger and, additionally, the unit definition in section 5.1.1. The maximum in specific heat demand corresponds to minimum temperatures in the cold outlet side in the heat recovery in the cross-flow heat exchanger. Since HEX-2 was set to operate with an outlet temperature of 55 °C, the heat to be provided to the stream to reach this temperature is normally higher for those with lower inlet temperature. It is complex though to analyze the direct effect of the parameter of interest - effect of solids formation - due to this coupling of the regeneration to the cross-flow heat exchanger resulting solely from the modelling.

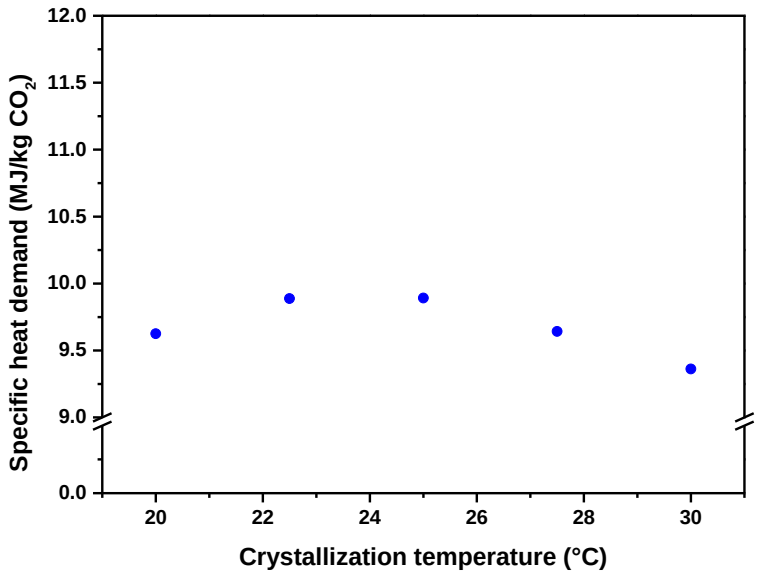

Figure 14. Specific heat demand sensitivity to crystallization temperatures

6.2.2. Absorber inlet temperature

The values defined in Table 7 are below the expected temperature for precipitation in the model. However, the solvent has at this point in the modelled system been regenerated and therefore, precipitation was not an issue since there is barely no CO_2 to push the chemistry towards solid formation.

The model predicts increased L/G for increased absorber inlet temperature. This trend is expected, since absorption for the AMP-NMP system is more effective at lower temperatures and, therefore, lower liquid circulation for the same gas inlet would be required. Additionally, it is possible to relate higher inlet temperatures in the absorber to lower amount of solid formation and the associated less material in the solid retained stream being regenerated. This was also expected as ions become diluted with more solvent circulating in the process, preventing chemical equilibrium leaning towards solid formation.

Regarding species loading throughout the process, the regenerated loading remains practically constant, whereas rich, solid concentrated and lean loadings present a slight decrease as the absorber inlet temperature is increased. The effect in the first two, rich and solid concentrated, is more noticeable than in the latter where the decrease is minimum.

The solid concentrated loading is a direct result of the rich loading, after temperature is decreased and solids are formed and filtered. The rich loading, itself, is directly related to the absorption. The change in the absorber inlet temperature has its major impact in this unit's performance via the different stages temperature and the related chemical equilibrium. Liquid phase temperature profiles in the absorber are presented in Figure 15. Stage 1 correspond to the upper stage, where the liquid enters and stage 30, to the gas inlet, the bottom stage. All profiles follow a similar trend, increasing between stages 1 to 10, staying quite stable between 10 and 27, after which temperature decreases until the end stage, 30. CO_2 loading present a similar profile, remarking the temperature effect on the chemical equilibrium (not shown here).

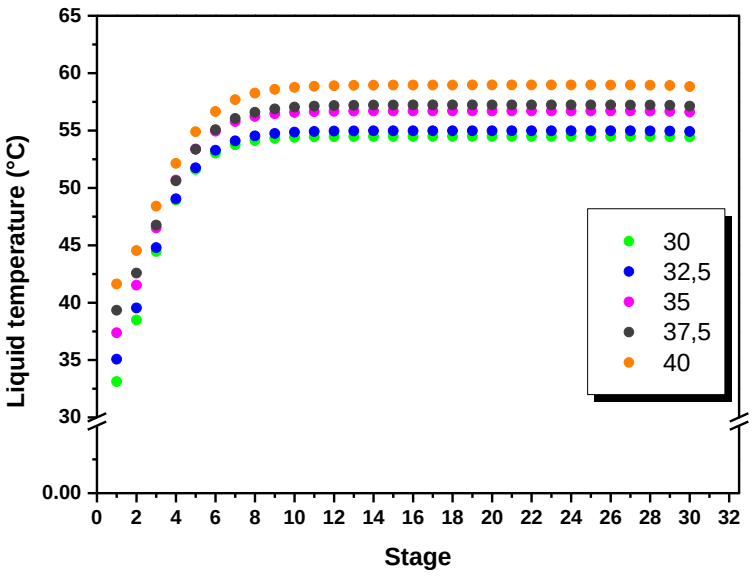

Figure 15. Absorber temperature profile for different absorber inlet temperatures

More liquid present in the stage to uptake heat released through chemical reactions, leads to the maintaining lower temperatures. This could explain why temperature profiles appeared to be closer between those inlet temperatures 30-32.5 and 35-37.5 since the L/G increase between those was greater than those between inlet temperatures 32.5-35, 37.5-40. The difference is most likely related to those numerical differences referred to in the beginning of section 6.2 regarding the design specification that calculates the liquid inlet.

Regarding the process energy requirements, results for different absorber inlet temperatures are shown in Figure 16. The absorber inlet temperature seems not to have any effect on the specific heat demand due to the basically constant value maintained around 9.85 MW/kg CO_2. This may be a result of the certain decoupling the filter brings to the process between absorption and desorption stages.

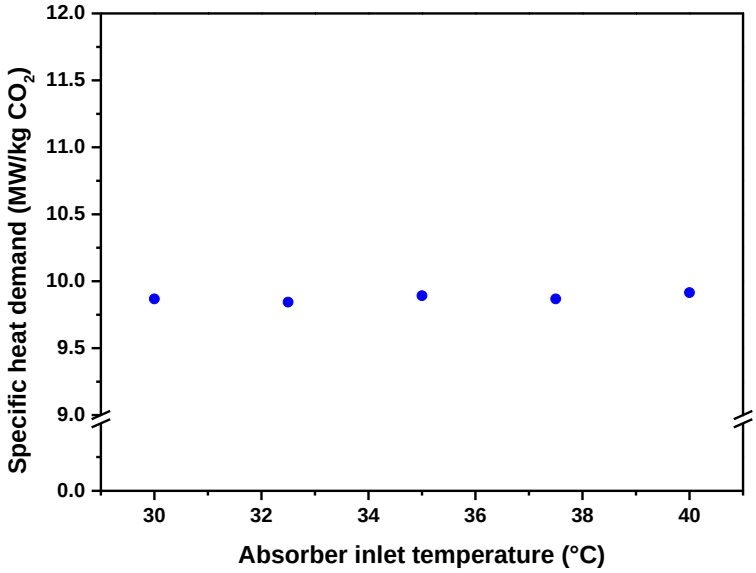

Figure 16. Specific heat demand sensitivity to absorber inlet temperatures

6.2.3. Slurry concentration in the retained solid

The most representative model variable in this case is the regenerated solvent ratio, i.e. how much material of the inlet material to the filter goes to the retained solid - from stream 5 to stream 6 in Figure 10. It is presented in Figure 17 for different slurry concentrations. It decreases as the slurry concentration is increased, with a hyperbolic character. The relationship solid concentration - regenerated solvent ratio is quite straightforward. If solid is concentrated more or less when sent to regenerate, the opposite occurs with the ratio filter inlet/retained solid streams, see section 5.1.1.

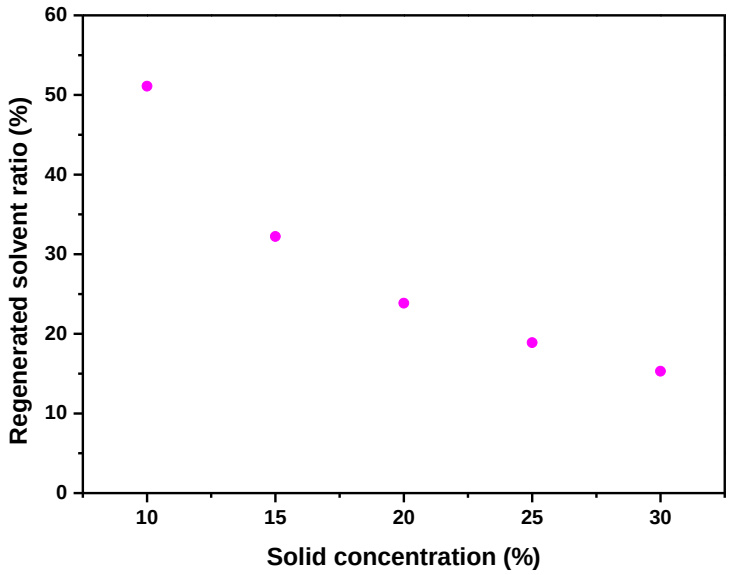

Figure 17. Regenerated solvent ratio sensitivity to solid concentrations

Changes in the L/G ratio are practically insignificant with a maximum difference of 1.6% when varying the solids concentration. This feature, as the specific heat demand in the previous case, also points towards the uncoupling absorption-desorption provided by the filtering stage.

Significant changes in CO_2 loadings can be seen in Figure 18. The most remarkable change is the solid concentrated loading, directly influenced by the solid concentration in the retained solid stream. The more the slurry is concentrated, the less liquid is sent to regeneration and therefore, the loading of this stream increases greatly as less NMP and unloaded AMP are part of it. Rich loadings experience minimum changes with a maximum difference of 1.3%, similar to the L/G ratios, highlighting their close relation. Regenerated and lean loadings both follow a trend alike the regenerated solvent split ratio, also closely related in process units, filter and stripper.

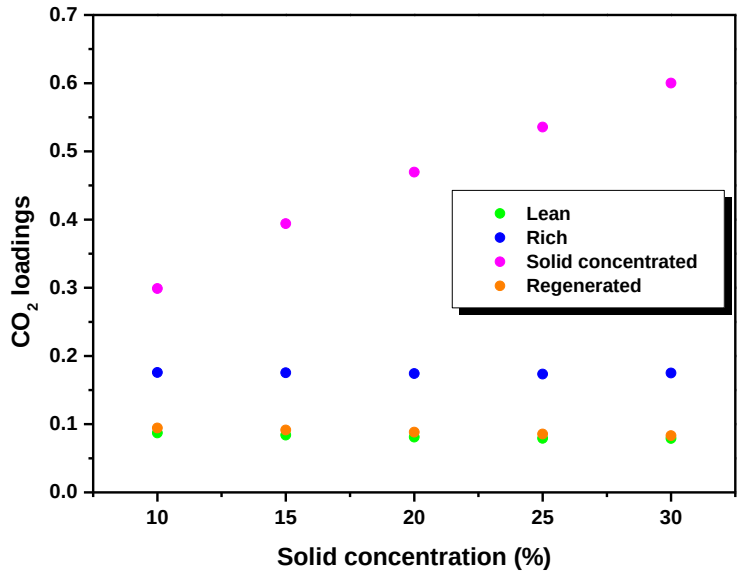

Figure 18. CO_2 loadings sensitivity to solid concentrations

Figure 19 shows the specific heat demand for the different solid concentrations in the retained solid. The lower specific heat requirements as slurry is concentrated can be related to the effect of heating less solvent and unloaded species. The trend is more remarkable between 10 and 15% solid concentration, similarly to reduction in regenerated solvent in Figure 17.

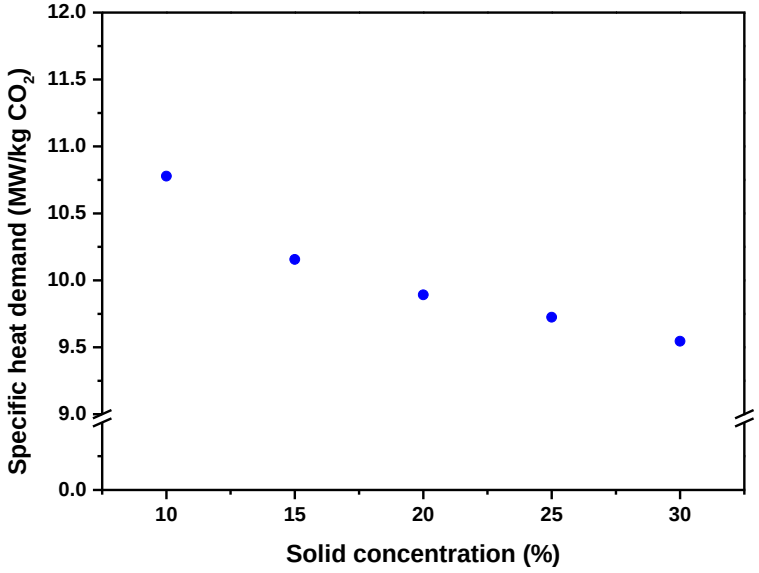

Figure 19. Specific heat demand sensitivity to solid concentrations

6.2.4. Regeneration temperature

The lower extent in the regeneration derived from the lower reboiler temperature, evidences in the regenerated loading, and impacts the process in several ways. First, loadings are increased as a result of the reduced ability to push the chemistry into gaseous CO_2 in the reboiler. These then impact the liquid circulation and regeneration requirements.

The effect on the L/G and the solvent regenerated ratio present a similar relationship. Both parameters present a decrease, with a slight hyperbolic character, as the reboiler temperature

increases. The reason for these trends is the CO_2 accumulation in the system, since smaller reboiler temperature also means reduced regeneration potential. This can be seen in the CO_2 loadings presented in Figure 20.

The most remarkable change is the difference in the regenerated loadings, going from being close to the lean for higher reboiler temperatures to close to rich loadings for reboiler temperatures close to 70 °C. Lean, rich and solid concentrated loadings also decrease as the reboiler temperature is decreased. However, the range in which they vary is much smaller. For the cases with 90 °C and 71 °C as reboiler temperature, the regenerated loading decreases by 127%. For which, rich loading, the next largest variation, only does by 20%.

Focusing on the regeneration side, where the inlet can be considered to be the solid concentrated and the outlet the regenerated streams. The difference in loadings between these two is decreased as the reboiler temperature decreases, highlighting the decreased regenerative potential. This is also related to the L/G since a system with lower regeneration, also has lower potential for up taking the incoming CO_2 in the feed gas and therefore, higher liquid circulation is required for a common gas to be treated.

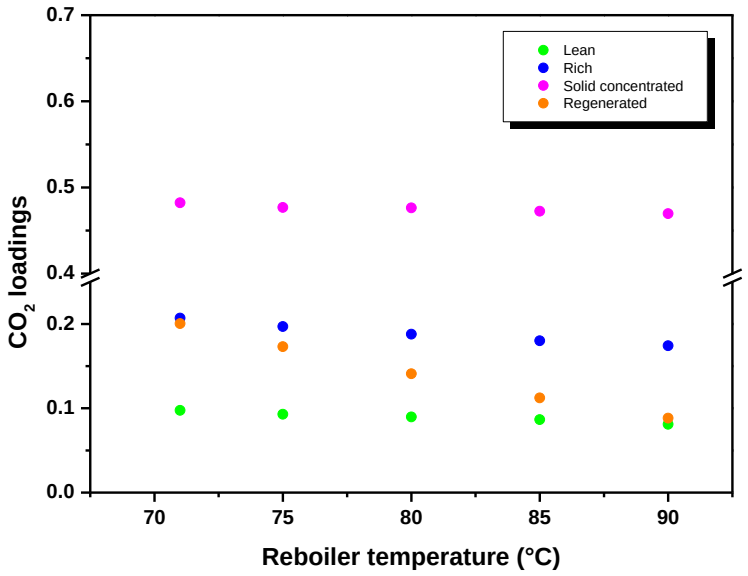

Figure 20. CO_2 loadings sensitivity to reboiler temperatures

Another aspect that must be considered is the impact in energy requirements. In Figure 21, specific heat demand for different reboiler temperatures is shown. It shows that decreasing the reboiler temperature increases the specific heat needed to capture CO_2. This is an interesting aspect, especially in this work where the regeneration temperatures make possible integration with process low-value waste heat. It is possible that reducing the temperature provides significant available heat so it is worth decreasing it. This balance between having more heat available and having a higher specific heat demand will be highly industry sector and site specific.

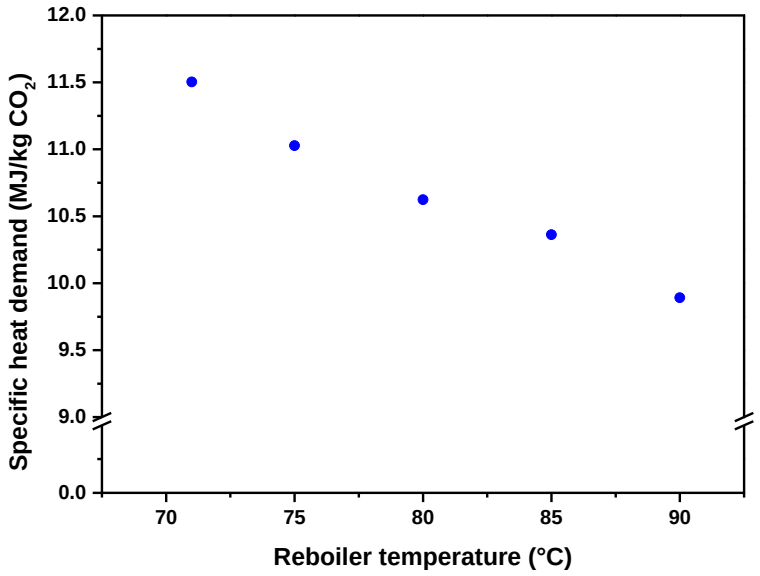

Figure 21. Specific heat demand sensitivity to reboiler temperatures

6.2.5. Capture rate

L/G ratios for the different capture rates are shown in Figure 22. It increases linearly with increased capture rate, which is usual since higher CO_2 to be captured requires higher solvent amounts to uptake it. Since L/G is directly determined by the liquid circulation set via design specification with a CO_2 outlet target.

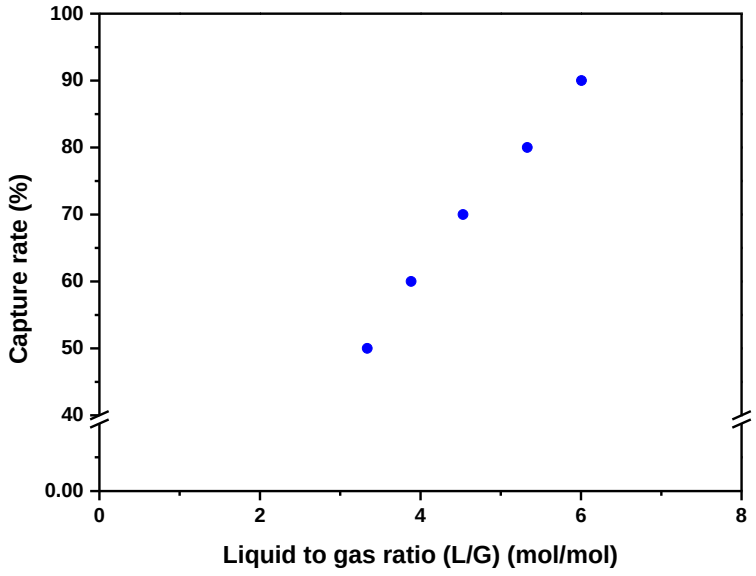

Figure 22. Capture rate sensitivity towards liquid to gas ratio

The regenerated ratio is practically constant around 24 mol% of the inlet to the filter. Additionally, no significant changes with the capture rate can be observed in the CO_2 loadings throughout the process. This is also noticed in the specific heat demand is presented in Figure 23, providing a similar outlook with no significant changes. It becomes thus clear that the capture target does not affect the process conditions rather the plant size determined through

the circulating solvent, which reflects in a similar trend in the change in the absorber diameter (Figure 23) to the one in Figure 22 for the L/G.

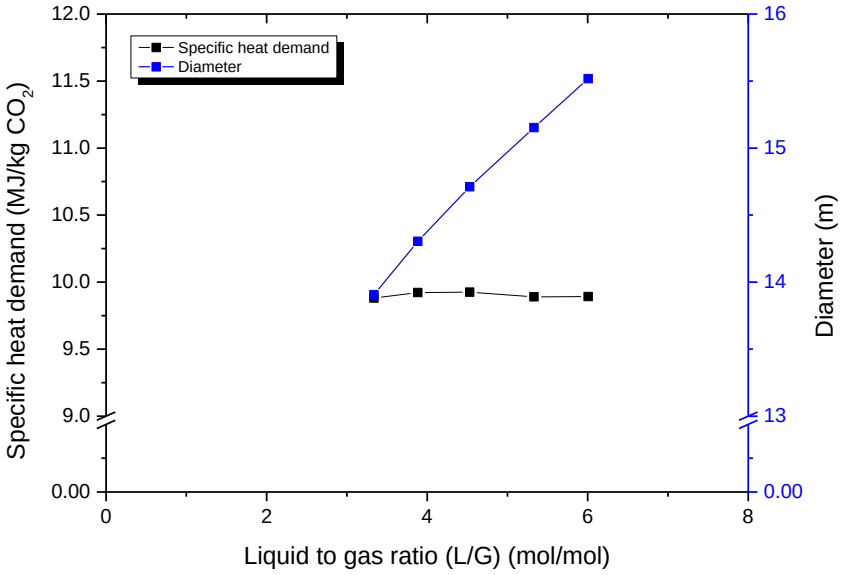

Figure 23. Absorber diameter and specific heat demand sensitivity to liquid to gas ratio

6.3. Case studies

6.3.1. Fixed capture rate

The base case organic AMP system was compared to aqueous MEA system for a capture efficiency of 90% from the blast furnace gas, cf. Table 5. The key performance indicators for both processes are shown in Table 11.

Table 11. Performance indicators for organic AMP and aqueous MEA processes

Parameter	Units	25 w% AMP in NMP	30 w% MEA in water
Lean loading	(mol/mol)	0.081	0.320
Rich loading	(mol/mol)	0.174	0.536
Liquid to gas ratio, L/G	(mol/mol)	6.01	9.14
Lean free amine*	mole frac.	0.334	0.041
Solvent circulation rate	kg/s	4550	1780
Column diameter	m	15.5	13.5
Column height	m	20.0	20.0
Mass transfer area	m^2	962000	727000
Specific heat demand	MJ/kg CO_2	9.89	3.78
Solvent slip - Clean gas	mole frac.	$8.54 \cdot 10^{-04}$	0.239
Amine slip - Clean gas	mole frac.	$5.83 \cdot 10^{-04}$	$8.42 \cdot 10^{-05}$
CO_2 purity	mole frac.	0.996	0.988
Solvent slip - CO_2-rich	mole frac.	0.002	0.012
Amine slip - CO_2-rich	mole frac.	0.001	$1.28 \cdot 10^{-12}$

*This term refers to the unbounded amine concentration in the absorber liquid inlet

When comparing AMP/MEA processes, the first two parameters coming to attention, due to their great differences, are lean and rich loadings. It is important to keep in mind that the CO_2 loading in AMP is limited through stoichiometry to be 1:2 (CO_2:AMP), whereas the CO_2 loading

of MEA defined in the same conditions is 1:1 (CO_2:MEA). AMP loading is even more limited in the modelled system since solid formation cannot occur in the absorber.

It may seem surprising that, regarding L/G ratio, there are less moles of solution required to uptake the same amount of CO_2, as both processes treat the same feed gas. The benchmark system has 30 w% MEA in water and the novel system 25 w% of AMP in NMP. However, regarding molar concentrations, since AMP is diluted in an organic solvent, with a similar molecular weight, its molar concentration in the absorber inlet is 33% (lean free amine in Table 11). This is not the case for MEA in aqueous dilution. The molecular weight of water is much smaller than for MEA, which results in the amine only presenting a molar concentration of 4.1%. Molecular weights also explain why there is much more solvent mass circulating in the organic system.

Solvent losses are much smaller for the organic system, both in the clean flue gas leaving the absorber and in the purified CO_2 stream. The overall AMP-NMP system presents lower volatility than the aqueous MEA system. It is also important to mention that the modelled MEA system included a condenser to generate a reflux to the stripper and recover MEA, which was not included in the AMP-NMP, which will likely reduce the losses even further once implemented. The lower volatility in the AMP-NMP system can be mostly related to the organic solvent since its boiling point is much lower than water's boiling point, 204 °C and 100 °C, respectively [96]. Additionally, the reboiler operates at much lower temperatures for AMP-NMP than NMP boiling point, whereas MEA is regenerated at 120 °C, higher than water boiling point. For the amines, the situation is not the same. In fact, more AMP is lost in both gaseous outlets. Moreover, AMP has a higher vapor pressure than MEA, 6 mm Hg vs 0.4 mm Hg at 25 °C, which makes this component more likely to go in the gaseous phase [97], [98]. However, all these parameters do not consider the interactions between system components so these should also be researched to formulate a clear conclusion.

The calculated absorber packing diameter, see section 5.1.1, is larger for AMP-NMP system. The limitations imposed by the solubility curve for the solid formation and, if this did not apply, Aspen Plus™ itself - see sections 4.4 and 5.1.2 -, lead to lower achievable rich loadings in the absorber than expectable. This results in lower cyclic capacity (rich/lean difference) and larger mass circulating. These influence the mass transfer, noticeable through the CO_2 loading profile - quite flat in the last stages - and, thus, the packing diameter seems to be as large as a result of hydraulics factors, to avoid the flooding through the column.

6.3.2. Industrially integrated with waste heat

Regarding the comparison on industrial performance, the NMP-AMP process was applied to reboiler temperatures of 75 °C and 90 °C. Results employing the actual cooling loading curve (ACLC) are presented in Table 12.

Table 12. Oil refinery case study integrated performance of CCS processes based on ACLC in the plant

Parameter	Units	AMP in NMP 75°C	AMP in NMP 90°C	MEA in water 120°C
Lean loading	(mol/mol)	0.087	0.076	0.330
Rich loading	(mol/mol)	0.194	0.168	0.541
Solid concentrated loading	(mol/mol)	0.448	0.446	-
Regenerated loading	(mol/mol)	0.172	0.085	-
Liquid to gas ratio, L/G	(mol/mol)	5.75	3.75	7.41
Absorber packing diameter	m	7.31	6.73	5.97
Absorber packing height	m	20.0	20.0	20.0
Mass transfer area	m^2	215,000	182,000	143,000
Specific heat demand	MJ/kg CO_2	11.1	9.89	3.75
Capture rate	(%)	79.5	63.5	73.4
Circulating solvent	kg/s	1050	675	340
Solvent slip - Clean gas	mole frac.	$9.11 \cdot 10^{-04}$	$1.50 \cdot 10^{-03}$	$2.25 \cdot 10^{-01}$
Amine slip - Clean gas	mole frac.	$7.16 \cdot 10^{-04}$	$1.27 \cdot 10^{-03}$	$3.09 \cdot 10^{-05}$
CO_2 purity	mol frac.	0.994	0.993	0.989
Solvent slip - CO_2-rich	mole frac.	$1.51 \cdot 10^{-03}$	$1.47 \cdot 10^{-03}$	$1.20 \cdot 10^{-02}$
Amine slip - CO_2-rich	mole frac.	$1.50 \cdot 10^{-03}$	$4.32 \cdot 10^{-03}$	$1.17 \cdot 10^{-12}$

The most relevant outcome from this industrial case are the possibilities that the organic AMP system offers in terms of heat integration. Even though the system presents much higher specific heat demand than the benchmark aqueous MEA, the possibility of reducing the reboiler temperature further unlocks much greater amounts of low-value waste heat in the current refinery operating conditions and, therefore, results in higher CO_2 captured, even though the specific heat requirements are more than 2.5 times larger.

The case for the MER network was also considered and results were obtained for both AMP-NMP as there would still be some heat available at 90 and 75 °C, which would result in CO_2 capture potential of 17.9 and 34.6%, respectively. In this case, aqueous MEA would not be a suitable system due to the lack of heat to integrate it with. However, it is important to notice that this network optimization was not done considering the construction of a CCS plant but instead optimized to improve energy efficiency. This means the AMP-NMP system may allow for CO_2 capture in cases where no other consumer, already on site, competes for heat of such temperature quality.

7. Conclusions

This Master's thesis has developed a process model of the 25w% AMP in NMP process for carbon capture. The model is able to describe the properties relevant, e.g. the characteristic solid precipitation of the AMP-NMP system. This is confirmed through comparison with experimental data of the system. However, precipitate still forms at lower temperatures than expected – about 33 °C compared to 55 °C. The process model is used to evaluate process performance through a sensitivity analyses and to compare it to the aqueous MEA process for a fixed capture rate and for a capture rate adjusted to the amount of available excess heat.

The results show that at the same design capture rate relative to the aqueous MEA-system the AMP-NMP system has:

- Larger circulating solvent mass (4550 kg/s relative to 1780 kg/s),
- Lower CO_2 loadings throughout the process (lean, 0.081; rich, 0.174; solid concentrated, 0.470 and regenerated, 0.088 relative to lean, 0.320 and rich, 0.536),
- Higher specific heat demand (9.89 vs 3.78 MJ/kg CO_2), and
- Lower solvent regeneration temperatures (71 - 90 °C relative to 120 °C)

In case of access to excess heat, the AMP-NMP system is a promising alternative as the possibility to regenerate the solvent at lower temperatures results in larger amounts of available heat to power solvent regeneration. Specifically in those cases where the excess heat at the lower regeneration temperature overcomes the higher specific heat demand relative to the aqueous-MEA system making the AMP-NMP system the better process.

In summary, the AMP in NMP is especially suitable for integration with existing plants with large amounts of excess heat in the range 110-90 °C. The process will also be favourable for a partial capture approach where only the amount of CO_2 possible to capture with available excess heat is utilized.

8. Future work

The work carried out in this Master thesis identifies four areas for future work: solid properties availability, chemical reactions, process modelling and technological deployment and industrial integration.

a) Regarding solid properties availability
   i. A new experimentally determined solubility curve is required. Through either a speciation to determine the chemical species in solution or pressure measurements – pressure can be related to CO_2 released into the gaseous phase - when performing the current experimental design in a closed system to isolate the solid dissolution.
   ii. Precipitated solid measurement for the CO_2 absorption analysis. Currently, the heat of solid formation has been estimated from these measurements and has a major impact on the specific heat demand in the process. It is a key parameter and, therefore, requires further improvement. These may come either from better estimations from the experimental data or via newly developed group contribution estimation techniques.
   iii. Determining the crystal growth behaviour and the particle size distribution. These properties affect the selection of the packing inside both the absorber and stripper as possible clogging should be avoided.

b) Regarding chemical reactions
   i. Modelling of the organic system as such. The AMP-NMP system is currently defined as "unsymmetric" in Aspen Plus™. Ideally, the proper symmetric definition could be accomplished by providing Aspen Plus™ with data regarding chemical reaction constants or the data for its regression.
   ii. Kinetics determination. It is of great importance to determine whether or not the kinetics limit the extent of the chemical reactions. It is relevant for understanding the system and also to its modelling.

c) Regarding process modelling
   i. By including a condenser on top of the stripper column in the AMP-NMP system, losses could be reduced and the purity of the CO_2 sent to compression further increased.
   ii. With the kinetics determination, given that they are the limiting factor, an equilibrium approach may be adopted for mass transfer in the column. This would allow for inter-stage solids in the columns (absorber and stripper), addressing one major limitation of the model developed in this work.
   iii. Pressure - temperature relation. The AMP-NMP system could also produce pressurized CO_2, which has been proven experimentally. However, this feature was not included in the current flow sheet, but may account for a major advantage for the AMP-NMP system. Including a pump after the filter and a valve before the cross-flow heat exchanger will additionally improve the heat transfer in this unit.

iv. The novel solvent system should be optimized separately without considering the benchmark aqueous MEA was design, i.e. tower height, stages, packing, etc.

d) Regarding technological deployment and industrial integration
   i. Process design and conditions need to be further researched to optimize the system performance.
   ii. Economical assessments should be carried out to determine what industries would be most likely to invest in the deployment of CCS system and, especially, in the novel solvent system. These should be site specific and coupled to the process excess heat available.
   iii. More case studies should be carried out targeting industrial CO_2 sources to expand the range of the system applicability.

References

[1] V. Andersson and H. Svensson, “Heat integration of a novel system for CCS at an oil refinery,” in *4th Post Combustion Capture Conference (PCCC4)*, 2017, pp. 8–10.

[2] J. Herrmann, “Process modeling of novel amine carbon capture solvents,” Norwegian University of Science and Technology, 2014.

[3] H. Svensson, C. Hulteberg, and H. T. Karlsson, “Precipitation of AMP carbamate in CO2 absorption process,” in *Energy Procedia*, 2014, pp. 750–757.

[4] S. Xu, Y.-W. Wang, F. D. Otto, and A. E. Mather, “Kinetics of the reaction of carbon dioxide with 2-amino-2-methyl-1-propanol solutions,” *Chem. Eng. Sci.*, vol. 51, no. 6, pp. 841–850, 1996.

[5] F. Barzagli, F. Mani, and M. Peruzzini, “Efficient CO2 absorption and low temperature desorption with non-aqueous solvents based on 2-amino-2-methyl-1-propanol (AMP),” *Int. J. Greenh. Gas Control*, vol. 16, pp. 217–223, 2013.

[6] C. Zheng, J. Tan, Y. J. Wang, and G. S. Luo, “CO2 solubility in a mixture absorption system of 2-amino-2-methyl-1-propanol with ethylene glycol,” *Ind. Eng. Chem. Res.*, vol. 52, no. 34, pp. 12247–12252, 2013.

[7] H. Karlsson and H. Svensson, “Regeneration of Non-Aqueous Precipitating Amine Solvents,” in *4th Post Combustion Capture Conference (PCCC4)*, 2017.

[8] S. Shahkarami, R. Azargohar, A. K. Dalai, and J. Soltan, “Breakthrough CO<inf>2</inf> adsorption in bio-based activated carbons,” *J. Environ. Sci. (China)*, vol. 34, pp. 68–76, 2015.

[9] S. Shahkarami, “CO2 CAPTURE FROM GASES USING ACTIVATED CARBON,” University of Saskatchewan, 2017.

[10] D. Y. C. Leung, G. Caramanna, and M. M. Maroto-Valer, “An overview of current status of carbon dioxide capture and storage technologies,” *Renew. Sustain. Energy Rev.*, vol. 39, pp. 426–443, 2014.

[11] UNFCCC, “Historic Paris Agreement on Climate Change - 195 Nations set path to keep temperature rise well below 2 degrees Celsius,” no. December. pp. 1–7, 2015.

[12] M. Wang and E. Oko, “Special issue on carbon capture in the context of carbon capture, utilisation and storage (CCUS),” *Int. J. Coal Sci. Technol.*, vol. 4, no. 1, pp. 1–4, 2017.

[13] IPCC, “Climate Change 2014 Synthesis Report Summary Chapter for Policymakers,” 2014.

[14] World Meteorological Organization, “WMO confirms 2017 among the three warmest years on record,” *Press Release Number: 18-01-2018*, 2018. [Online]. Available: https://public.wmo.int/en/media/press-release/wmo-confirms-2017-among-three-warmest-years-record.

[15] W. Schakel, “Understanding Environmental Trade-Offs of Carbon Capture, Utilization and Storage,” Utrecht University, 2017.

[16] GEA, “Global Energy Assessment,” 2012.

[17] S. Fuss, J. G. Canadell, G. P. Peters, M. Tavoni, R. M. Andrew, P. Ciais, R. B. Jackson, C. D. Jones, F. Kraxner, N. Nakicenovic, C. Le Quéré, M. R. Raupach, A. Sharifi, P. Smith, and Y. Yamagata, "Betting on negative emissions," *Nat. Clim. Chang.*, vol. 4, no. 10, pp. 850–853, 2014.

[18] IEA, "World Energy Outlook 2016," *Int. Energy Agency*, pp. 1–8, 2016.

[19] K. Riahi, E. Kriegler, N. Johnson, C. Bertram, M. den Elzen, J. Eom, M. Schaeffer, J. Edmonds, M. Isaac, V. Krey, T. Longden, G. Luderer, A. Méjean, D. L. McCollum, S. Mima, H. Turton, D. P. van Vuuren, K. Wada, V. Bosetti, P. Capros, P. Criqui, M. Hamdi-Cherif, M. Kainuma, and O. Edenhofer, "Locked into Copenhagen pledges - Implications of short-term emission targets for the cost and feasibility of long-term climate goals," *Technol. Forecast. Soc. Change*, vol. 90, pp. 8–23, 2015.

[20] U.S. Energy Information Administration, "Annual Energy Outlook 2015," *Off. Integr. Int. Energy Anal.*, vol. 1, pp. 1–244, 2015.

[21] B. Caldecott, G. Lomax, and M. Workman, "Stranded carbon assets and negative emissions technologies," *Smith Sch. Enterp. Environ. Univ. Oxford*, vol. 2, no. February, pp. 1–37, 2015.

[22] S. Budinis, N. Mac Dowell, S. Krevor, T. Dixon, J. Kemper, and A. Hawkes, "Can Carbon Capture and Storage Unlock 'Unburnable Carbon'?," *Energy Procedia*, vol. 114, no. November 2016, pp. 7504–7515, 2017.

[23] IEA, "Technology roadmap - Carbon capture and Storage," 2013.

[24] A. Al-Mamoori, A. Krishnamurthy, A. A. Rownaghi, and F. Rezaei, "Carbon Capture and Utilization Update," *Energy Technology*. 2017.

[25] M. E. Boot-Handford, J. C. Abanades, E. J. Anthony, M. J. Blunt, S. Brandani, N. Mac Dowell, J. R. Fernández, M.-C. Ferrari, R. Gross, J. P. Hallett, R. S. Haszeldine, P. Heptonstall, A. Lyngfelt, Z. Makuch, E. Mangano, R. T. J. Porter, M. Pourkashanian, G. T. Rochelle, N. Shah, J. G. Yao, and P. S. Fennell, "Carbon capture and storage update," *Energy Environ. Sci.*, vol. 7, no. 1, pp. 130–189, 2014.

[26] M. Wang, A. Lawal, P. Stephenson, J. Sidders, and C. Ramshaw, "Post-combustion CO2capture with chemical absorption: A state-of-the-art review," *Chem. Eng. Res. Des.*, vol. 89, no. 9, pp. 1609–1624, 2011.

[27] E. S. Rubin, J. E. Davison, and H. J. Herzog, "The cost of CO2 capture and storage," *Int. J. Greenh. Gas Control*, vol. 40, pp. 378–400, 2015.

[28] Bert Metz, O. Davidson, H. de Coninck, M. Loos, and L. Meyer, "IPCC special report on carbon dioxide capture and storage," 2005.

[29] Y. Kong, X. Shen, M. Fan, M. Yang, and S. Cui, "Dynamic capture of low-concentration CO2 on amine hybrid silsesquioxane aerogel," *Chem. Eng. J.*, vol. 283, pp. 1059–1068, 2016.

[30] B. Arstad, H. Fjellvåg, K. O. Kongshaug, O. Swang, and R. Blom, "Amine functionalised metal organic frameworks (MOFs) as adsorbents for carbon dioxide," *Adsorption*, vol. 14, no. 6, pp. 755–762, 2008.

[31] S. Builes, P. López-Aranguren, J. Fraile, L. F. Vega, and C. Domingo, "Analysis of CO2

adsorption in amine-functionalized porous silicas by molecular simulations," *Energy and Fuels*, vol. 29, no. 6, pp. 3855–3862, 2015.

[32] A. Goeppert, M. Czaun, R. B. May, G. K. S. Prakash, G. A. Olah, and S. R. Narayanan, "Carbon dioxide capture from the air using a polyamine based regenerable solid adsorbent," *J. Am. Chem. Soc.*, vol. 133, no. 50, pp. 20164–20167, 2011.

[33] P. Markewitz, W. Kuckshinrichs, W. Leitner, J. Linssen, P. Zapp, R. Bongartz, A. Schreiber, and T. E. Müller, "Worldwide innovations in the development of carbon capture technologies and the utilization of CO2," *Energy Environ. Sci.*, vol. 5, no. 6, pp. 7281–7305, 2012.

[34] D. M. Ruthven, *Principles of adsorption and adsorption processes*. John Wiley & Sons, 1984.

[35] L. Hauchhum and P. Mahanta, "Carbon dioxide adsorption on zeolites and activated carbon by pressure swing adsorption in a fixed bed," *Int. J. Energy Environ. Eng.*, vol. 5, no. 4, pp. 349–356, 2014.

[36] S. Choi, J. H. Drese, and C. W. Jones, "Adsorbent materials for carbon dioxide capture from large anthropogenic point sources," *ChemSusChem*, vol. 2, no. 9, pp. 796–854, 2009.

[37] A. Agarwal, L. T. Biegler, and S. E. Zitney, "A superstructure-based optimal synthesis of PSA cycles for post-combustion CO2 capture," *AIChE J.*, vol. 56, no. 7, pp. 1813–1828, 2010.

[38] J. Merel, M. Clausse, and F. Meunier, "Experimental investigation on CO2 post−combustion capture by indirect thermal swing adsorption using 13X and 5A zeolites," *Ind. Eng. Chem. Res.*, vol. 47, no. 1, pp. 209–215, 2008.

[39] A. L. Chaffee, G. P. Knowles, Z. Liang, J. Zhang, P. Xiao, and P. A. Webley, "CO2 capture by adsorption: materials and process development," *Int. J. Greenh. gas Control*, vol. 1, no. 1, pp. 11–18, 2007.

[40] D. Marx, L. Joss, M. Hefti, and M. Mazzotti, "Temperature swing adsorption for postcombustion CO2 capture: single-and multicolumn experiments and simulations," *Ind. Eng. Chem. Res.*, vol. 55, no. 5, pp. 1401–1412, 2016.

[41] T. Takeguchi, W. Tanakulrungsank, and T. Inui, *Separation and/or concentration of CO2 from CO2/N2 gaseous mixture by pressure swing adsorption using metal-incorporated microporous crystals with high surface area*, vol. 7, no. 1. Elsevier, 1993.

[42] J. Karger and D. M. Ruthven, "Diffusion in Zeolites and Other Microporous Solids Wiley-Interscience," *New York*, 1994.

[43] G. Li, P. Xiao, P. A. Webley, J. Zhang, and R. Singh, "Competition of CO2/H2O in adsorption based CO2 capture," *Energy Procedia*, vol. 1, no. 1, pp. 1123–1130, 2009.

[44] D. M. Ruthven, S. Farooq, and K. S. Knaebel, "Pressure Swing Adsorption VCH," *New York*, 1994.

[45] M. M. Hossain and H. I. de Lasa, "Chemical-looping combustion (CLC) for inherent CO2 separations—a review," *Chem. Eng. Sci.*, vol. 63, no. 18, pp. 4433–4451, 2008.

[46] R. T. Symonds, D. Y. Lu, V. Manovic, and E. J. Anthony, “Pilot-scale study of CO2 capture by CaO-based sorbents in the presence of steam and SO2,” *Ind. Eng. Chem. Res.*, vol. 51, no. 21, pp. 7177–7184, 2012.

[47] N. Rodríguez, M. Alonso, and J. C. Abanades, “Experimental investigation of a circulating fluidized-bed reactor to capture CO2 with CaO,” *AIChE J.*, vol. 57, no. 5, pp. 1356–1366, 2011.

[48] A. Charitos, C. Hawthorne, A. R. Bidwe, S. Sivalingam, A. Schuster, H. Spliethoff, and G. Scheffknecht, “Parametric investigation of the calcium looping process for CO2 capture in a 10 kWth dual fluidized bed,” *Int. J. Greenh. Gas Control*, vol. 4, no. 5, pp. 776–784, 2010.

[49] E. Oko, M. Wang, and A. S. Joel, “Current status and future development of solvent-based carbon capture,” *Int. J. Coal Sci. Technol.*, 2017.

[50] IEAGHG, “Assessment of Emerging CO2 Capture Technologies and Their Potential,” 2014.

[51] S. Bolat, “Technology Readiness Level (TRL) put into practice,” 2016. [Online]. Available: https://serkanbolat.com/2016/02/17/technology-readiness-level-trl-put-into-practice/.

[52] S. Chi and G. T. Rochelle, “Oxidative degradation of monoethanolamine,” *Ind. Eng. Chem. Res.*, vol. 41, no. 17, pp. 4178–4186, 2002.

[53] I. J. Uyanga and R. O. Idem, “Studies of SO2-and O2-induced degradation of aqueous MEA during CO2 capture from power plant flue gas streams,” *Ind. Eng. Chem. Res.*, vol. 46, no. 8, pp. 2558–2566, 2007.

[54] J. Davis and G. Rochelle, “Thermal degradation of monoethanolamine at stripper conditions,” *Energy Procedia*, vol. 1, no. 1, pp. 327–333, 2009.

[55] J. Kittel, R. Idem, D. Gelowitz, P. Tontiwachwuthikul, G. Parrain, and A. Bonneau, “Corrosion in MEA units for CO2 capture: pilot plant studies,” *Energy Procedia*, vol. 1, no. 1, pp. 791–797, 2009.

[56] H. P. Mangalapally, R. Notz, S. Hoch, N. Asprion, G. Sieder, H. Garcia, and H. Hasse, “Pilot plant experimental studies of post combustion CO2 capture by reactive absorption with MEA and new solvents,” *Energy Procedia*, vol. 1, no. 1, pp. 963–970, 2009.

[57] Alstom, “Alstom announces successful results of Mountaineer Carbon Capture and Sequestration (CCS) Project.,” 2011. [Online]. Available: http://www.alstom.com/press-centre/2011/5/alstom-announces-sucessful-results-of-mountaineer-carbon-capture-and-sequestration-ccs-project/.

[58] R. Faber, M. Köpcke, O. Biede, J. N. Knudsen, and J. Andersen, “Open-loop step responses for the MEA post-combustion capture process: Experimental results from the Esbjerg pilot plant,” *Energy Procedia*, vol. 4, pp. 1427–1434, 2011.

[59] F. Seibert, E. Chen, M. Perry, S. Briggs, R. Montgomery, and G. Rochelle, “UT/SRP CO2 capture pilot plant—Operating experience and procedures,” *Energy Procedia*, vol. 4, pp. 1616–1623, 2011.

[60] M. Rabensteiner, G. Kinger, M. Koller, and C. Hochenauer, “Three years of working

experience with different solvents at a realistic post combustion capture pilot plant," *Energy Procedia*, vol. 63, pp. 1578–1584, 2014.

[61] CO2 Technology Centre Mongstad (TCM), "About TCM." [Online]. Available: http://www.tcmda.com/en/About-TCM/.

[62] A. Cousins, L. T. Wardhaugh, and P. H. M. Feron, "A survey of process flow sheet modifications for energy efficient CO2 capture from flue gases using chemical absorption," *Int. J. Greenh. Gas Control*, vol. 5, no. 4, pp. 605–619, 2011.

[63] H. Ahn, M. Luberti, Z. Liu, and S. Brandani, "Process configuration studies of the amine capture process for coal-fired power plants," *Int. J. Greenh. Gas Control*, vol. 16, pp. 29–40, 2013.

[64] J. Oexmann, *Post-combustion CO2 capture: energetic evaluation of chemical absorption processes in coal-fired steam power plants*. Technische Universität Hamburg, 2011.

[65] G. Sartori and D. W. Savage, "Sterically hindered amines for carbon dioxide removal from gases," *Ind. Eng. Chem. Fundam.*, vol. 22, no. 2, pp. 239–249, 1983.

[66] K. S. Fisher, K. Searcy, G. T. Rochelle, S. Ziaii, and C. Schubert, "Advanced amine solvent formulations and process integration for near-term CO2 capture success," Trimeric Corporation, 2007.

[67] L. Dubois and D. Thomas, "Screening of aqueous amine-based solvents for postcombustion CO2 capture by chemical absorption," *Chem. Eng. Technol.*, vol. 35, no. 3, pp. 513–524, 2012.

[68] V. Darde, K. Thomsen, W. J. M. Van Well, and E. H. Stenby, "Chilled ammonia process for CO2 capture," *Int. J. Greenh. Gas Control*, vol. 4, no. 2, pp. 131–136, 2010.

[69] J. P. Brouwer, P. H. M. Feron, and N. A. M. Ten Asbroek, "Amino-acid salts for CO2 capture from flue gases," in *Fourth annual conference on carbon capture & sequestration*, 2005, vol. 5.

[70] L. Raynal, P. Alix, P.-A. Bouillon, A. Gomez, M. le F. de Nailly, M. Jacquin, J. Kittel, A. di Lella, P. Mougin, and J. Trapy, "The DMX^{TM} process: an original solution for lowering the cost of post-combustion carbon capture," *Energy Procedia*, vol. 4, pp. 779–786, 2011.

[71] B. Zacchello, E. Oko, M. Wang, and A. Fethi, "Process simulation and analysis of carbon capture with an aqueous mixture of ionic liquid and monoethanolamine solvent," *Int. J. Coal Sci. Technol.*, vol. 4, no. 1, pp. 25–32, 2017.

[72] B. M. Lerche, E. H. Stenby, and K. Thomsen, "CO2 capture from flue gas using amino acid salt solutions," *Dep. Chem. Biochem. Eng. Tech. Univ. Denmark, Denmark*, 2012.

[73] A. K. Chakraborty, G. Astarita, and K. B. Bischoff, "CO2 absorption in aqueous solutions of hindered amines," *Chem. Eng. Sci.*, vol. 41, no. 4, pp. 997–1003, 1986.

[74] H. Svensson, *Energy Efficient Processes for the Production of Gaseous Biofuels-Reforming and Gas Upgrading*. Department of Chemical Engineering, Lund University, 2014.

[75] F. Bougie and M. C. Iliuta, "Sterically hindered amine-based absorbents for the removal of CO2 from gas streams," *J. Chem. Eng. Data*, vol. 57, no. 3, pp. 635–669, 2012.

[76] J.-Y. Park, S. J. Yoon, and H. Lee, “Effect of steric hindrance on carbon dioxide absorption into new amine solutions: thermodynamic and spectroscopic verification through solubility and NMR analysis,” *Environ. Sci. Technol.*, vol. 37, no. 8, pp. 1670–1675, 2003.

[77] C. Zheng, J. Tan, Y. J. Wang, and G. S. Luo, “CO2 Solubility in a Mixture Absorption System of 2-Amino-2-methyl-1-propanol with Glycol,” *Ind. Eng. Chem. Res.*, vol. 51, no. 34, pp. 11236–11244, 2012.

[78] E. Jo, Y. H. Jhon, S. B. Choi, J.-G. Shim, J.-H. Kim, J. H. Lee, I.-Y. Lee, K.-R. Jang, and J. Kim, “Crystal structure and electronic properties of 2-amino-2-methyl-1-propanol (AMP) carbamate,” *R. Soc. Chem.*, 2010.

[79] H. Svensson, J. Edfeldt, V. Z. Velasco, C. Hulteberg, and H. T. Karlsson, “Solubility of carbon dioxide in mixtures of 2-amino-2-methyl-1-propanol and organic solvents,” *Int. J. Greenh. Gas Control*, vol. 27, pp. 247–254, 2014.

[80] M. Sanku and H. Svensson, “Crystallization Kinetics of AMP Carbamate in Solutions of AMP in Organic Solvents NMP or TEGDME,” in *Energy Procedia*, 2017, vol. 114, pp. 840–851.

[81] J. Gabrielsen, H. F. Svendsen, M. L. Michelsen, E. H. Stenby, and G. M. Kontogeorgis, “Experimental validation of a rate-based model for CO2 capture using an AMP solution,” *Chem. Eng. Sci.*, vol. 62, no. 9, pp. 2397–2413, 2007.

[82] J. Xiao, C.-W. Li, and M.-H. Li, “Kinetics of absorption of carbon dioxide into aqueous solutions of 2-amino-2-methyl-1-propanol+ monoethanolamine,” *Chem. Eng. Sci.*, vol. 55, no. 1, pp. 161–175, 2000.

[83] K. Al-Malah, “Electrolytes,” in *Aspen Plus Chemical Engineering Applications*, 2017, pp. 301–324.

[84] M. Sanku and H. Svensson, “Solid precipitation data,” *Unpubl. data*.

[85] H. Karlsson and H. Svensson, “Heat of absorption data,” *Unpubl. data*.

[86] Molecular Knowledge Systems Inc., “Cranium Software.” [Online]. Available: http://www.molecularknowledge.com/Cranium/cranium.htm.

[87] A. Technology, “Aspen Physical Property Methods,” 2013.

[88] H. Svensson, V. Zejnullahu Velasco, C. Hulteberg, and H. T. Karlsson, “Heat of absorption of carbon dioxide in mixtures of 2-amino-2-methyl-1-propanol and organic solvents,” *Int. J. Greenh. Gas Control*, vol. 30, pp. 1–8, 2014.

[89] F. Barzagli, C. Giorgi, F. Mani, and M. Peruzzini, “Reversible carbon dioxide capture by aqueous and non-aqueous amine-based absorbents: A comparative analysis carried out by13C NMR spectroscopy,” *Appl. Energy*, vol. 220, no. March, pp. 208–219, 2018.

[90] S. O. Garðarsdóttir, F. Normann, K. Andersson, and F. Johnsson, “Postcombustion CO2 capture using monoethanolamine and ammonia solvents: The influence of CO2 concentration on technical performance,” *Ind. Eng. Chem. Res.*, vol. 54, no. 2, pp. 681–690, 2015.

[91] M. Sanku and H. Svensson, “Modelling CO2 capture with AMP in NMP system,” in *4th*

Post Combustion Capture Conference (PCCC4), 2017.

[92] R. Skagestad, F. Normann, S. Ó. Garðarsdóttir, M. Sundqvist, M. Anheden, N. H. Eldrup, H. Ali, H. A. Haugen, and A. Mathisen, "CO2stCap-Cutting Cost of CO2 Capture in Process Industry," *Energy Procedia*, vol. 114, pp. 6303–6315, 2017.

[93] S. O. Gardarsdottir, F. Normann, K. Andersson, and F. Johnsson, "Process evaluation of CO2 capture in three industrial case studies," *Energy Procedia*, vol. 63, no. 0, pp. 6565–6575, 2014.

[94] M. Sanku, H. Karlsson, and H. Svensson, "AMP in NMP / TEGDME for post-CCS," in *9th Trondheim Conference on Carbon Capture, Transport and Storage*, 2017.

[95] F. Barzagli, C. Giorgi, F. Mani, and M. Peruzzini, "Direct Air Capture (DAC) of CO2 accomplished by different alkanolamines," in *International Conference on Negative CO2 Emissions*, 2018.

[96] EASTMAN, "N-Methyl-2-Pyrrolidone (NMP)," *Material Safety Data Sheet*. [Online]. Available: https://www.eastman.com/Pages/ProductHome.aspx?product=71103627.

[97] PubChem Open Chemistry Database, "Monoethanolamine." [Online]. Available: https://pubchem.ncbi.nlm.nih.gov/compound/Ethanolamine#section=Ecological-Information. [Accessed: 01-Jun-2018].

[98] PubChem Open Chemistry Database, "Aminomethylpropanol." [Online]. Available: https://pubchem.ncbi.nlm.nih.gov/compound/11807#section=Melting-Point. [Accessed: 01-Jun-2018].

[99] M. D. Hilliard, "A Predictive Thermodynamic Model for an Aqueous Blend of Potassium Carbonate, Piperazine, and Monoethanolamine for Carbon Dioxide Capture from Flue Gas," *Dr. thesis Tech. Univ. Texas Austin*, p. 1083, 2008.

Appendix 1. Minimum component parameter definition

When introducing components in Aspen Plus™ as custom defined, there are certain parameter requirements. Scalar parameters for molecules and ions are presented in Table 13 and Table 14, respectively. Temperature dependent parameters can be found in Table 15 for molecules and in Table 16 for ions.

Table 13. Molecule scalar parameter definition

DGFORM	Standard free energy of formation for ideal gas at 25 °C
DHFORM	Standard enthalpy of formation for ideal gas at 25 °C
DHVLB	Enthalpy of vaporization at TB
MW	Molecular weight
OMEGA	Pitzer acentric factor
PC	Critical pressure
RKTZRA	Parameter for the Rackett liquid molar volume model
TB	Normal boiling point
TC	Critical temperature
VC	Critical temperature
ZC	Critical compressibility factor

Table 14. Ion scalar parameter definition

CHARGE	Ionic Charge number (positive for cations, negative for anions)
DGAQFM*	Aqueous phase free energy of formation at infinite dilution and 25 °C. For ionic species and molecular solutes in electrolyte systems
DHAQFM*	Aqueous phase heat of formation at infinite dilution and 25 °C. For ionic species and molecular solutes in electrolyte systems
MW	Molecular weight
RADIUS	Born radius of ionic species
ZWITTER	Identifies zwitterions; Set the parameter to 1 for a zwitterion and 0 for other components.

* For ionic species and molecular solutes in electrolyte systems

Table 15. Molecule temperature dependent parameters

CPDIEC	Pure component dielectric constant coefficients of non-aqueous solvents
CPIG or CPIGDP	Ideal gas heat capacity
DHVLWT or DHVLDP	Vaporization equation for pure components
PLXANT	Coefficients for the Extended Antoine vapor pressure equation for a liquid
VLBROC	Brelvi-O-Connell Volume Parameter

Table 16. Ion temperature dependent parameters

CPAQ0	Aqueous phase heat capacity at infinite dilution polynomial
PLXANT	Coefficients for the Extended Antoine vapor pressure equation for a liquid
VLBROC	Brelvi-O-Connell Volume Parameter

Appendix 2. Method selection

Both considered methods, “ELECNRTL” and “ENRTL-RK”, were expected to deliver the same results since the system considered is a single solid and single electrolyte system as neither water equilibrium nor the zwitterion formation through equilibrium are included in the definition. However, they did not and to discriminate between them, the method choice was based on how the performance of each in the simulation environment related to the actual results observed in the experimental results.

The whole open-loop system (

Figure 24) was run employing both methods for all units. However, the analysis towards selection was focused around the first blocks, “NMP-ABS” and “HEX”.

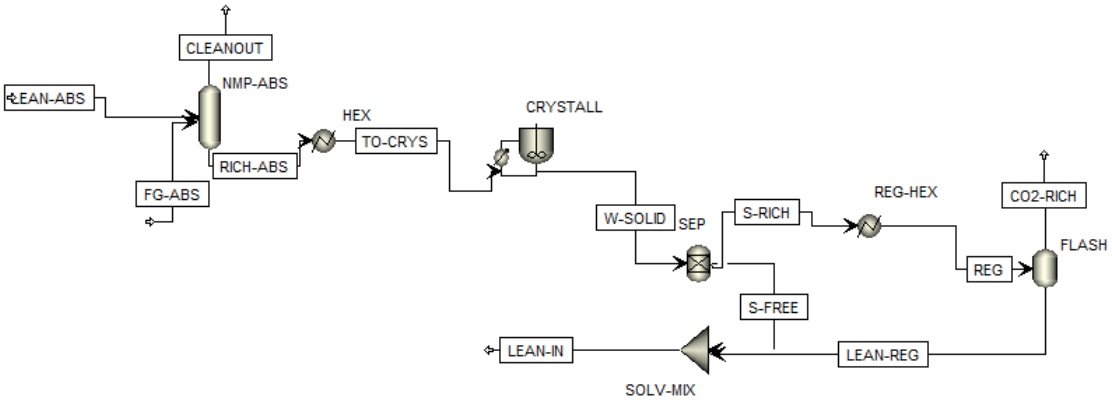

Figure 24. Open-loop process simulation

First, it was realized that the use of different method affects the absorption stage. The streams leaving the system are not the equal nor are the temperature profiles inside. In terms of capturing potential, “ENRTL-RK” results were better since the chemistry appeared to be shifted more towards the ionic species formation rather than presenting most of the CO_2 just physically absorbed which was resulting from “ELECNRTL” application. The relevant species composition for the outlet stream “RICH-ABS” in Figure 24, with common settings for the inlets and block definition, are presented in Table 17.

Table 17. Absorption liquid outlet different “RICH-ABS” composition

Component	“ENRTL-RK” outlet (kmol/s)	“ELECNRTL” outlet (kmol/s)
AMP	11.6	14.8
CO2	0.138	0.100
$AMPH^+$	1.58	0.005
AMPCOO-	1.58	0.005
SOLID	0	0

Since temperature profiles observed were also differing for both methods, the possibility of this affecting the capturing rate and equilibrium was considered. For “ENRTL-RK”, temperatures were in the range 58-68°C whereas for “ELECNRTL”, were stable around 50°C. As

an attempt to try to overcome this difference, the amine solution temperature was increase which in turn did not influence much the results.

The next step was the evaluation of a mix method, in which absorption calculations were performed under “ENRTL-RK” and the “HEX” block instead was set to apply “ELECNRTL”. In this case, it became clear that the latter method presents a poorer performance when it comes to stabilizing ions in solution. This was motivated from the great difference in ionic concentration between the inlet and outlet streams when temperature is decreased from around 68 to 50 ºC (Table 18).

Table 18. Ionic and representative components load change after “HEX”

Component	“RICH-ABS” (kmol/s)	“TO-CRYS” (kmol/s)
AMP	11.6	12.4
CO2	0.154	0.527
AMPH$^+$	1.608	0.008
AMPCOO-	1.608	0.008
SOLID	0	1.226

It becomes therefore clear that ions cannot be held with “ELECNRTL” and instead the extra concentration of this sort of compound is directed into either dissolved CO_2 and amine or solid formation. In addition to this, results showed that solid formation occurs in all systems. However, it is important to note that when methods are mixed, using “ENRTL-RK” for the absorption column and “ELECNRTL” as GLOBAL method, i.e. for the rest of the units, the crystal formation occurs at much higher temperatures, around 50 °C whereas in single method systems temperature must be at least 25 °C to observe precipitation. The fact that precipitation temperature is closer to that previously reported in [3] when employing a mixed method is not due to a better representation. It is mainly due to the already mentioned inability of “ELECNRTL” to hold the ions generated in the absorption through “ENRTL-RK” application. Therefore, if used, the overall system would not be properly described.

Since experimental results showed that the system has a good ability to stabilize the ions in solution, therefore applying “ENRTL-RK” has base method accounts for better representation of the actual overall system behaviour.

Appendix 3. Zwitterion modelling

Aspen Plus™ incorporates methods to estimate properties through group contribution. These can be classified according to the extent of the effect accounted for, e.g. Joback is a first-order method whereas Benson is a second-order one, which considers the effect of neighbouring atoms. It is, though, as expected much more complex but also delivers more accurate results [87]. Moreover, not all methods can be employed for all parameters estimating nor the same inputs are required for each method when estimating a certain value. An example for vapor pressure estimation is presented in Table 19.

Table 19. Method required input for group contribution vapor pressure estimation

Method	Information required	Recommended use
Data	Vapor pressure data	-
Riedel	TB, TC, PC, (vapor pressure data)	Nonpolar compounds
Li-Ma	Structure, TB, (vapor pressure data)	Polar and nonpolar compounds
Mani	PC, (vapor pressure data) (also uses TC if available)	Complex compounds that decompose at temperatures below the normal boiling points

The first and most basic step is to incorporate the compound's structure so that its intramolecular bonds can be calculated, presented in Figure 25. It contains the correct charges, however the groups defined to contribute to the parameter estimation did not cover COO^- or NH_2^+, which were estimated as COOH and NH, respectively.

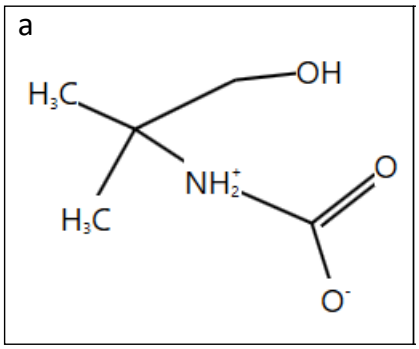

Figure 25. Zwitterion structure definition

Zwitterion estimated properties and those defined in the initial model proposed in [80] for this system were carefully checked. As expected, the parameters that could have not been calculated involved those related to the reaction equilibrium and the heat released, i.e. the aqueous phase free energy of formation (DGAQFM) and the aqueous phase heat of formation (DHAQFM), both at infinite dilution and 25 °C, which are also for molecular species in solution. These parameters cannot be estimated through group contribution. Therefore, it was decided to implement those from the initial model as user defined parameters, listed in Table 20.

Table 20. Parameters retrieved for the zwitterion

Parameter	DGAQFM	DHAQFM
Value (kcal/mol)	-65.511	-123.061

Speciation

Speciation refers to the varying concentrations, the split in the forms a certain compound can present. In this case, the species in solution relative to Reactions 1 to 4, see 2.3.2.1, were analysed as a function of the solvent medium temperature. The main reason behind the speciation calculations and the discard of the zwitterion as a component influencing the system. With this approximation, it was possible to reduce a complex and highly variable reaction which greatly affected the convergence of the solution.

A minor setting that must be included also in the process simulation is to select a true-component approach so composition in the results is expressed in terms of ions, salts and molecular species rather than just in base components resulting from an apparent-component approach. Information was retrieved from Aspen Plus™. An absorber with 2 stages was defined for this purpose, to which inlets were defined as the base flue gas considered in this thesis and a 25% weight AMP in NMP as solvent. From this, the outlet liquid stream information was extracted, temperature and required species flow. To have a different outlet stream temperature, the inlet temperatures for both gas and liquid were varied in a sensitivity analysis between 15 and 60°C with a 2.5°C increment. Different inlet stream temperatures affect the temperature profile inside the 2-stage column. Therefore, as an attempt to minimize this possible effect on the speciation results, only temperature multiple of 5, with a ±1°C range for which a mean value was calculated, were considered. Speciation results are presented in Figure 26. It was clear that the zwitterion would not have a significance presence in the system and could, therefore, be excluded from the modelling.

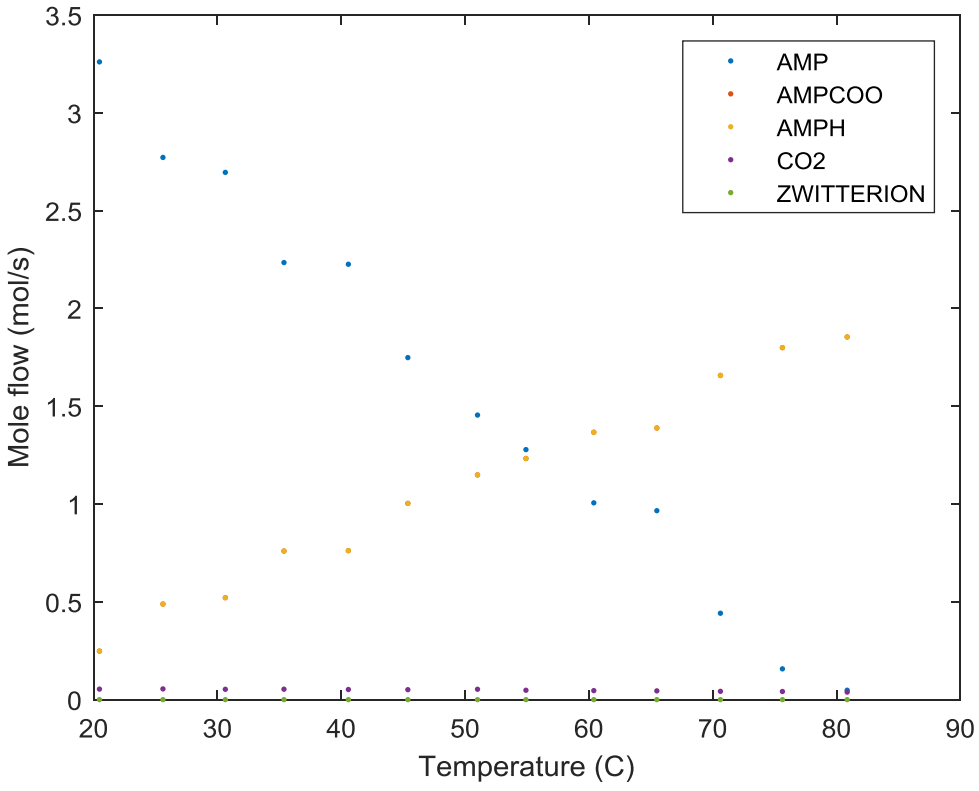

Figure 26. Ion speciation

Limitations

Regarding the way in which the zwitterion was handled, there are certain limitations

- Group contribution

When specifically considering charges, these can only be included for inorganic compounds with Mostafa contribution method. As previously mentioned, COO^- and NH_3^+ groups were estimated as COOH and NH_2, respectively, and different contribution group methods employed. This definition does not account for the electronic distribution in the compound. However, since the compound is also defined with a charge equal zero, the electronic interactions are most likely more restricted due to this aspect. To avoid this restriction, several references mention the possibility of including a small charge into the zwitterion, 1e-5 [2], [99]. However, in this master thesis this is not considered as it leads to charge imbalances in the system when the zwitterion reacts.

- Speciation

Property

Properties underlying in the zwitterion definition that mainly influence the speciation correspond to those for piperazine one. These properties are the aqueous phase free energy of formation and the aqueous phase heat of formation, both at infinite dilution and 25 °C. These parameters define the equilibrium constant for the reaction and the heat released in such, respectively. The speciation is therefore likely not properly corresponding to what occurs. However, it was the closest possible option as the compound to which has been approximated is of the same type. Removing the zwitterion from the components present in the system due to its low concentration is therefore considered valid.

Block selection

Selecting an absorption for the speciation calculations presents certain drawbacks. The impact of these in the results as mentioned before was limited in certain way. However, temperature profiles affect greatly the absorption and therefore, the amount of CO_2 and ionic species that can be formed in the following stage. Therefore, it was possible to observe different speciation and component shares at close temperatures because of this effect. This was especially remarkable at lower temperatures.

An alternative block definition that was considered was RGibbs. However, it could not have been employed for this purpose since it considers only the separate values provided directly as Gibbs energy rather than considering the chemistry as well for its internal calculations. Therefore, this cannot be used when the solid is also considered.

Appendix 4. Solubility regression

Data regression to determine the best fit including different combinations of the possible significant parameters presented in Equation 1.

A summary with the most relevant information for the selection is presented in Table 21. The check on model parameters from the individual statistical data was done in most convenient order, higher R-squared values first until acceptable 95% confidence limits.

Table 21. Data regression summary

Case	R-squared	Adjusted R-squared	Parameter limits (95% confidence)
ABCD	0.963	0.951	Non-acceptable
ABC	0.952	0.936	-
ACD	0.954	0.938	Acceptable
ABD	0.953	0.937	-
AB	0.902	0.888	-
AC	0.888	0.873	-
AD	0.874	0.856	-

Further detailed information can be found for the specific case results below. The confidence intervals for all the cases are not shown. However, the reader could be able to calculate them from the statistical data provided.

- Case ABCD

$$\ln K_{eq} = A + \frac{B}{T} + C\ln(T) + D \cdot T \qquad \text{(A.1)}$$

Table 22 presents the results in relation to the individual contribution of the parameters to the model, whereas Table 23 presents the results in relation to the significance of the model itself.

Table 22. Parameter statistical results for ABCD case

Parameter	Value estimate	Standard Error (SE)	t-Statistic (tStat)	Statistical p-Value
A	-28900	288	-100	$6.62 \cdot 10^{-11}$
B	$7.91 \cdot 10^{05}$	10.5	75500	$3.64 \cdot 10^{-28}$
C	5010	60.0	83.5	$1.98 \cdot 10^{-10}$
D	-7.83	0.181	-43.2	$1.03 \cdot 10^{-08}$

Table 23. Model statistical results for ABCD case

Number of observations	9
Error degrees of freedom	6
Root Mean Squared Error	0.332
R-Squared	0.963
Adjusted R-Squared	0.951
F-statistic vs. constant model	78.8
p-value	$4.93 \cdot 10^{-05}$

- Case ABC

$$\ln K_{eq} = A + \frac{B}{T} + C \ln(T) \quad \text{(A.2)}$$

Table 24 presents the results in relation to the individual contribution of the parameters to the model, whereas Table 25 presents the results in relation to the significance of the model itself.

Table 24. Parameter statistical results for ABC case

Parameter	Value estimate	SE	tStat	pValue
A	1190	467	2.55	0.043
B	-63900	22600	-2.82	0.030
C	-172	68.6	-2.51	0.046

Table 25. Model statistical results for ABC case

Number of observations	9
Error degrees of freedom	6
Root Mean Squared Error	0.38
R-Squared	0.952
Adjusted R-Squared	0.936
F-statistic vs. constant model	59.6
p-value	$1.10 \cdot 10^{-04}$

- Case ACD

$$\ln K_{eq} = A + C \ln(T) + D \cdot T \quad \text{(A.3)}$$

Table 26 presents the results in relation to the individual contribution of the parameters to the model, whereas Table 27 presents the results in relation to the significance of the model itself.

Table 26. Parameter statistical results for ACD case

Parameter	Value estimate	SE	tStat	pValue
A	-1070	324	-3.29	0.017
C	217	67.5	3.22	0.018
D	-0.592	0.204	-2.91	0.027

Table 27. Model statistical results for ACD case

Number of observations	9
Error degrees of freedom	6
Root Mean Squared Error	0.373
R-Squared	0.954
Adjusted R-Squared	0.938
F-statistic vs. constant model	61.8
p-value	$9.92 \cdot 10^{-05}$

- Case ABD

$$\ln K_{eq} = A + \frac{B}{T} + D \cdot T \quad \text{(A.4)}$$

Table 28 presents the results in relation to the individual contribution of the parameters to the model, whereas Table 29 presents the results in relation to the significance of the model itself.

Table 28. Parameter statistical results for ABD case

Parameter	Value estimate	SE	tStat	pValue
A	192	68.2	2.82	0.030
B	-35600	11200	-3.17	0.019
D	-0.263	0.103	-2.55	0.043

Table 29. Model statistical results for ABD case

Number of observations	9
Error degrees of freedom	6
Root Mean Squared Error	0.377
R-Squared	0.953
Adjusted R-Squared	0.937
F-statistic vs. constant model	60.6
p-value	$1.05 \cdot 10^{-04}$

- Case AB

$$\ln K_{eq} = A + \frac{B}{T} \quad \text{(A.5)}$$

Table 30 presents the results in relation to the individual contribution of the parameters to the model, whereas Table 31 presents the results in relation to the significance of the model itself.

Table 30. Parameter statistical results for AB case

Parameter	Value estimate	SE	tStat	pValue
A	18.2	2.59	7.01	$2.09 \cdot 10^{-04}$
B	-7000	874	-8.01	$9.04 \cdot 10^{-05}$

Table 31. Model statistical results for AB case

Number of observations	9
Error degrees of freedom	7
Root Mean Squared Error	0.504
R-Squared	0.902
Adjusted R-Squared	0.888
F-statistic vs. constant model	64.2
p-value	$9.04 \cdot 10^{-05}$

- Case AC

$$\ln K_{eq} = A + C\ln(T) \tag{A.6}$$

Table 32 presents the results in relation to the individual contribution of the parameters to the model, whereas Table 33 presents the results in relation to the significance of the model itself.

Table 32. Parameter statistical results for AC case

Parameter	Value estimate	SE	tStat	pValue
A	-125	16.4	-7.62	$1.24 \cdot 10^{-04}$
C	21.1	2.82	7.47	$1.41 \cdot 10^{-04}$

Table 33. Model statistical results for AC case

Number of observations	9
Error degrees of freedom	7
Root Mean Squared Error	0.536
R-Squared	0.888
Adjusted R-Squared	0.873
F-statistic vs. constant model	55.8
p-value	$1.41 \cdot 10^{-04}$

- Case AD

$$\ln K_{eq} = A + D \cdot T \tag{A.7}$$

Table 34 presents the results in relation to the individual contribution of the parameters to the model, whereas Table 35 presents the results in relation to the significance of the model itself.

Table 34. Parameter statistical results for AD case

Parameter	Value estimate	SE	tStat	pValue
A	-24.0	3.08	-7.77	$1.10 \cdot 10^{-04}$
D	0.063	$9.07 \cdot 10^{-03}$	6.96	$2.19 \cdot 10^{-04}$

Table 35. Model statistical results for AD case

Number of observations	9
Error degrees of freedom	7
Root Mean Squared Error	0.570
R-Squared	0.874
Adjusted R-Squared	0.856
F-statistic vs. constant model	48.5
p-value	$2.19 \cdot 10^{-04}$

Appendix 5. Detailed solid heat of formation estimation

Since additional reactions are happening in parallel to the one of interest, the solid formation, in the system measured, see Reaction 1-4 in 2.3.2.1. The solid heat of formation had to be estimated from measurements covering all of these in [85] since no other estimation method provided this parameter. Considering the modelled system, a similar situation to the one in the experimental set up in [88] occurs in the crystallizer block, see Figure 10 in section 5.1.1. Solid precipitates in this block for the first time and, additionally, ions and CO_2 can be absorbed from the gaseous phase into the solution. Therefore, the modelled crystallizer block seems comparable to the experimental set up in [3] and a reasonable basis for estimating the solid heat of formation.

In the modelled crystallizer, solids appear for the first time in the system, which was related to the experimentally observed sudden precipitation in the heat of absorption measurement, as shown in Figure 27. Therein, the amount of measured heat release is related to the CO_2 loading in solution. The sudden heat release increase at about 0.2 CO_2 loading corresponds to the solid precipitation. The magnitude of this was related to the possible prior supersaturation state of the solution, which lead to additional solid precipitation that had already been formed at lower loadings (previous points). However, even though the heat measured in this point is then greater that what could be expected, it represents the best point for the estimation. The measured points once the solid has precipitated (the bulk of the solid has precipitated) do not necessarily correspond to further solid precipitation, they could rather be related to crystal growth. Therefore, they may not serve as an actual representation of the solid heat of formation.

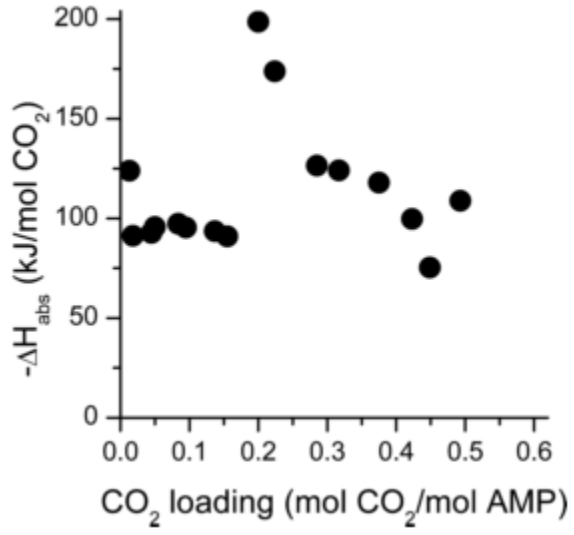

Figure 27. Heat of absorption in 25 w% AMP in NMP at 50 °C [88]

The amount of crystal formed could not be determined in the experiments since the current set-up does not allow for such measurements as crystals cannot be extracted without disrupting the whole system and modifying chemical equilibrium. Therefore, it was considered that the complete amount of CO_2 absorbed (100%) went into solid formation. This was an

optimistic approach, meaning the amount of heat released per solid was minimized as the amount of crystals formed was maximized.

Using the assumption on crystal formation, the heat corresponding to the solid precipitation reaction can be separated from the rest. Checking the prior experimental points where no solid had precipitated, it was possible to determine how much heat corresponds to ion formation and physical absorption per mole CO_2 taken into the solution in each point. The heat released per absorbed mole of CO_2 was considered that of the heat for ion formation and physical absorption was equal to that observed in the previous experimental point; see the blue square in Figure 28. Then, the contribution from the solid was isolated, which in Figure 28 is represented by the green square.

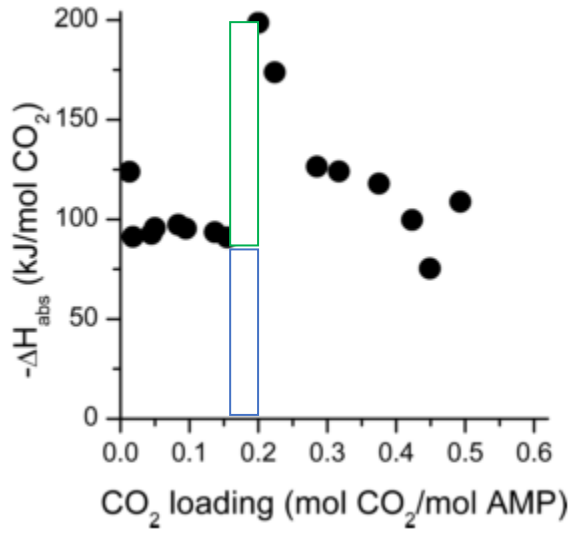

Figure 28. Share of heat related to the solid formation in the estimation

By now, the experimental data and the point to check the estimation are determined. However, this check point is not the direct parameter Aspen Plus™ takes as an input. Therefore, an initial estimation was required. A simulation was run and then, the heat requirements in the modelled crystallizer can be compared to those in the experimental data. With the mismatch, the estimation of the solid heat of formation, the property parameter, was adjusted until proper correspondence was achieved.

In this procedure explanation, data at 50 °C has been presented. However, the actual data employed for the calculation was at 40 °C, since it was the temperature closer to the crystallizer operation, in which precipitation occurred at 33 °C.

Appendix 6. Cranium™ estimated AMP carbamate properties

Again, the first step for its use is the solid structure definition. The program requires for the compounds present to be completely linked forming a unique structure, meaning it is not possible to define the solid as two separate ions; instead an ionic link is included. This results in the solid structure shown in Figure 29.

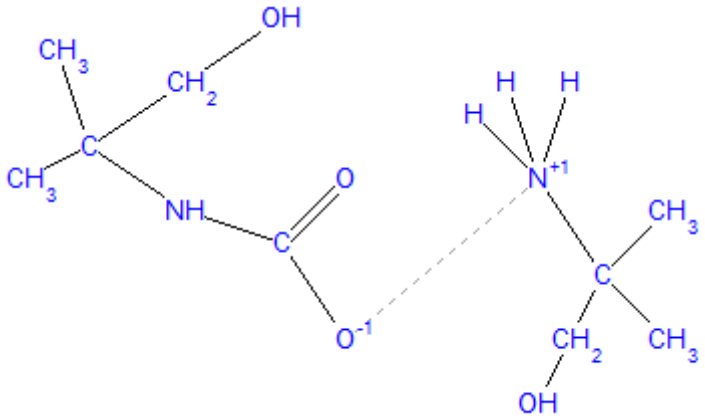

Figure 29. Cranium solid AMP carbamate structure definition

For this structure, the software cannot estimate all required parameters, only the solid heat capacity. However, it was enough to complete the property requirements as the rest were calculated from experimental data. Values for the properties estimated, units and methods can be found in Table 36.

Table 36. Properties estimation for AMP Carbamate when employing structure 1

Property	Value	Units	Technique
Constant Properties Section			
Molecular weight (MW)	$2.20 \cdot 10^{02}$	-	Definition
Acentric factor (Acf)	$-2.43 \cdot 10^{-01}$	-	Definition
Critical Properties Section			
Critical temperature (Tc)	$3.48 \cdot 10^{02}$	K	Wilson + Jasperson Method - First Order
Critical pressure (Pc)	$1.35 \cdot 10^{06}$	Pa	Vapor Pressure Extrapolation
Zc	$3.11 \cdot 10^{-02}$	-	Definition
Thermodynamic Properties Section			
ΔHfL,298	$1.25 \cdot 10^{05}$	J/kg	Vapor Estimate Adjustment
CpS,298	$1.61 \cdot 10^{03}$	J/kgK	Hurst + Harrison
Phase Transition Enthalpies Section			
ΔHvap	$5.41 \cdot 10^{04}$	J/kg	Vetere Method

Appendix 7. Kinetics implementation effect

Kinetics data was available for the aqueous MEA-based process. The performance of the absorber is compared for having reactions set to equilibrium and having them defined by kinetics. The effect was expected to be more significant in this block since it is where all reactions related to the CO_2 chemical absorption occur. The comparison is hold between the liquid inlet and outlet for both cases. The inlet flue gas is common as well as the capturing target set to 90% inlet CO_2. Stream flows, composition and temperature are shown in Table 37. It was clear that when a kinetics approach was employed a greater amount of solvent was required to achieve the same capturing rate of 90%. This means chemistry kinetics became the limiting factor when included for the MEA-based system. Both lean inlets are quite similar in component mole fractions, which allows for rough direct comparison of the rich outlets after the absorption since both were implemented in the same column design to the same flue gas inlet. Two reaction sets apply in aqueous MEA-based CO_2 capture, the carbonic acid ions formation and the MEA loading with CO_2. Applying kinetics seems to favour the acid formation reactions, which can be taken from the much higher CO_3^{2-} formation in the chemistry kinetically calculated outlet. Whereas for MEA reactions, kinetic calculations do not favour the loaded specie formation.

Table 37. Kinetics effect in MEA-based calculations

	Lean inlet to absorber		**Rich outlet from absorber**	
Reaction mode	**Kinetic**	**Equilibrium**	**Kinetic**	**Equilibrium**
Temperature (°C)	40.0	40.0	57.9	51.1
Mole flow (kmol/s)	83.4	73.0	82.8	71.3
Component mole fraction				
MEA	0.041	0.041	0.008	0.002
H_2O	0.886	0.886	0.874	0.873
CO_2	$5.21 \cdot 10^{-08}$	$5.21 \cdot 10^{-08}$	$4.54 \cdot 10^{-05}$	$7.88 \cdot 10^{-05}$
H_3O^+	$5.61 \cdot 10^{-12}$	$5.61 \cdot 10^{-12}$	$1.56 \cdot 10^{-10}$	$3.73 \cdot 10^{-10}$
OH^-	$7.13 \cdot 10^{-06}$	$7.13 \cdot 10^{-06}$	$1.16 \cdot 10^{-06}$	$3.54 \cdot 10^{-07}$
HCO_3^-	$3.47 \cdot 10^{-04}$	$3.47 \cdot 10^{-04}$	0.010	0.010
CO_3^{2-}	0.001	0.001	0.003	0.001
$MEAH^+$	0.037	0.037	0.060	0.063
$MEACOO^-$	0.034	0.034	0.045	0.050

However, AMP-based system is completely different so there is no clear conclusion on how implementing the kinetics would affect the system performance. Unlike MEA system, AMP in NMP is an organic system in which it is not possible for CO_2 to react with water into carbonic ion formation, since water is absent. This means there is no competition with any other species formation.